

EFFECT OF CORRECTIVE SURGERY ON LOWER LIMB MECHANICS IN
PATIENTS WITH CROUCH GAIT

by

Adelle Milholland



A thesis

submitted in partial fulfillment

of the requirements for the degree of

Master of Science in Mechanical Engineering

Boise State University

December 2019

© 2019

Adelle Milholland

ALL RIGHTS RESERVED

BOISE STATE UNIVERSITY GRADUATE COLLEGE

DEFENSE COMMITTEE AND FINAL READING APPROVALS

of the thesis submitted by

Adelle Milholland

Thesis Title: Effect of Corrective Surgery on Lower Limb Mechanics in Patients with Crouch Gait

Date of Final Oral Examination: 02 September 2019

The following individuals read and discussed the thesis submitted by student Adelle Milholland, and they evaluated the student's presentation and response to questions during the final oral examination. They found that the student passed the final oral examination.

Clare K. Fitzpatrick, Ph.D. Chair, Supervisory Committee

Trevor Lujan, Ph.D. Member, Supervisory Committee

Gunes Uzer, Ph.D. Member, Supervisory Committee

The final reading approval of the thesis was granted by Clare K. Fitzpatrick, Ph.D., Chair of the Supervisory Committee. The thesis was approved by the Graduate College.

DEDICATION

This work is dedicated to my parents whose faith in me is humbling. I could not be where I am today without their unwavering support.

ACKNOWLEDGEMENTS

My thesis advisor, Dr. Clare Fitzpatrick, has been an invaluable source of assistance and guidance. I cannot express the extent of my gratitude for her help and patience. I would also like to thank my committee, Dr. Lujan and Dr. Uzer, they have been a source of learning and encouragement throughout my years as a graduate student.

ABSTRACT

Crouch gait is a progressively degrading gait deviation associated with the neurological disorder cerebral palsy. If left untreated it can lead to anterior knee pain and a loss of ambulation. At present there exists no agreed upon metric for determining the surgical procedures used to treat crouch gait and there is insufficient means to analytically compare the results of different procedures. The aims of this thesis work were to create a pipeline to transform a patient's gait analysis data into a finite element model, develop a model of sufficient complexity to evaluate a range of outcomes by which to judge the efficacy of a surgical procedure, analyze the change between pre- and post-operative models and the changes between models with different surgical procedures, and to quantify the impact of varying different surgical parameters.

A generic lower limb rigid body musculoskeletal model was developed and used in conjunction with patient-specific static and dynamic motion capture to create scaling factors and joint kinematics, respectively. The musculoskeletal model was scaled and converted into a finite element model. This lower torso model was integrated with a detailed finite element model of the knee joint including patella, femur and tibia heads, associated articular cartilage, patellofemoral ligaments, patellar tendon, and quadriceps tendons. This type of combined finite element model was created for each patient, pre- and post-operatively, for a series of patient's treated for crouch gait at Children's Hospital Colorado. Each model was modified to replicate the surgical procedure(s) that each individual patient underwent. Comparison between pre- and post-operative models

show significant improvement in tibiofemoral flexion-extension and patellar articular cartilage stress in post-operative models.

In order to assess the effect of surgical parameters on muscle efficiency, the finite element model was modified such that tibiofemoral flexion-extension was controlled by adaptive muscle forces calculated using a proportional-integral feedback control system. The feedback system adjusted quadriceps and hamstrings forces to try and meet a target flexion profile. A feedback control model was created for three patients; subsequently, each model was modified to run multiple simulations with modified surgical procedures and parameters. The models were modified to include distal femoral extension osteotomy procedures of 0°, 15°, or 30°, or patella tendon advancement procedures with 0 cm, 1 cm, or 2 cm shortening. The muscle forces needed to reach the target kinematics were compared. Further simulations are required to identify clear links between surgical decisions and patient-specific parameters, but the developed model shows promise for future studies both for crouch gait and other musculoskeletal pathologies.

TABLE OF CONTENTS

DEDICATION	iv
ACKNOWLEDGEMENTS	v
ABSTRACT	vi
LIST OF FIGURES	x
LIST OF ABBREVIATIONS	xii
CHAPTER ONE: INTRODUCTION	1
1.1 Motivation.....	1
1.2 Research Goals.....	4
CHAPTER TWO: MODEL DEVELOPMENT.....	8
2.1 Clinical Data Collection	8
2.2 Rigid-Body Musculoskeletal Model	9
2.3 Kinematics	11
2.4 Knee Finite Element Model.....	14
2.5 Lower Extremity Finite Element Model.....	15
2.6 Proportional-Integral Controlled Muscles	16
2.7 Model Application	19
CHAPTER THREE: MANUSCRIPT “EFFECT OF CORRECTIVE SURGERY ON LOWER LIMB MECHANICS IN PATIENTS WITH CROUCH GAIT”	20
3.1 Introduction.....	20
3.2 Methods	24

3.3 Results	29
3.4 Discussion.....	32
CHAPTER FOUR: PROPORTIONAL INTEGRAL FEEDBACK CONTROL AND THE PARAMETRIC ASSESSMENT OF SURGICAL DECISIONS	34
4.1 Introduction.....	34
4.2 Methods	35
4.3 Results	37
4.4 Discussion.....	47
CHAPTER FIVE: CONCLUSIONS	49
5.1 Summary.....	49
5.2 Limitations	50
5.3 Future Work.....	51
REFERENCES.....	53

LIST OF FIGURES

Figure 1	Pre- (left) and post- (right) operative rigid-body musculoskeletal model in OpenSim during gait cycle simulation 11
Figure 2	Left femur geometry with DP and ML axes and the nodes used to create said axes 12
Figure 3	Exploded view of tibiofemoral joint coordinate system axes (Naendrup, Zlotnicki, Murphy, Patel, Debski, & Musahl, 2019)..... 13
Figure 4	Right hip joint coordinate system axes 13
Figure 5	Sagittal (left), frontal (middle), and angled (right) view of lower extremity finite element model 16
Figure 6	Comparison of target and achieved tibiofemoral flexion-extension angle for three patients 18
Figure 7	Finite element model: combined model (left) and detailed knee (right) ... 25
Figure 8	Detailed knee finite element model used for patients treated with PTA pre-surgery (left) and post-surgery (right) 28
Figure 9	X-ray (left), edge detection (middle), and lines for angle calculation (right) 28
Figure 10	Tibiofemoral flexion-extension kinematics pre- and post-operative; lagging leg (left) and leading leg (right) 30
Figure 11	90th percentile von mises stress pre- and post-operative; lagging leg (left) and leading leg (right) 30
Figure 12	Contact area of patellar articular cartilage pre- and post-operative; lagging leg (left) and leading leg (right) 31
Figure 13	Stress on patellar articular cartilage of same patient pre- (Left) and post-operatively (Right) 31
Figure 14	Tibiofemoral flexion-extension kinematics pre-operative; lagging leg (left) and leading leg (right) 32

Figure 15	Pathological (left) and healthy (right) patella tendon.....	37
Figure 16	Radiograph after DFEO (A), edge detection (B), and lines used for baseline DFEO angle (C).....	37
Figure 17	Total quadriceps force calculated by the proportional integral control system for a single model	39
Figure 18	Target and actual tibiofemoral flexion kinematics.....	40
Figure 19	Total quadriceps force from PI muscle control and inverse dynamics with static optimization	41
Figure 20	Total quadriceps forces for models with varying baseline DFEO angle ...	42
Figure 21	Maximum quadriceps force from swing phase for models with differencing DFEO angles (* indicates patient's actual surgery)	44
Figure 22	Initial position of knee joint for DFEO models with baseline angles; 0° (left), 15° (middle), and 30° (right)	45
Figure 23	Maximum quadriceps force from swing phase for PTA models. Patient surgery; proximal tendon resection (top), distal tendon resection (middle), and imbrication (bottom)	46
Figure 24	Initial position of knee joint for PTA models with varying lengths of Tendon Shortening; 2cm shortening (left), 1cm shortening (middle), and no shortening (right)	47

LIST OF ABBREVIATIONS

AP	Anterior-posterior
CP	Cerebral palsy
DFEO	Distal femoral extension osteotomy
DOF	Degrees of freedom
DP	Distal-proximal
EMG	Electromyography
FE	Finite element
FEM	Finite element methods
ML	Medial-lateral
PTA	Patellar tendon advancement
PF	Patellofemoral
PI	Proportional Integral
ROM	Range of motion
SEMLS	Single event multi-level surgery
TF	Tibiofemoral

CHAPTER ONE: INTRODUCTION

1.1 Motivation

Cerebral palsy is a neurological disorder found in roughly 0.36% of children in the US (Yeargin-Allsopp, Braun, Doernberg, Benedict, Kirby, & Durkin, 2008). Crouch gait is one of the most common gait deviations found in patients with cerebral palsy (Rethlefsen, Blumstein, Kay, Dorey, & Ray, 2016). Crouch gait is characterized by an excessive amount of flexion at the knee joint during gait. It is a progressively degrading gait deviation, in part because the crouched posture itself reduces the capacity for muscles to generate extension accelerations at the hip and knee joints (Hicks, Schwartz, Arnold, & Delp, 2008).

Over time, a patient's gait can decay to the point where they are non-ambulatory and require assistive devices such as a walker or wheelchair to move around. Current treatment for these advanced stages of crouch gait involves surgical intervention. Single event multi-level surgery (SEMLS) has been accepted as the preferred method to treat musculoskeletal deformities and gait deviations in patients with cerebral palsy and has been proven to provide both short and long term improvement (Lamberts et al., 2016; Öunpuu, Solomito, Bell, Deluca, & Pierz, 2015). The surgical procedures included in the SEMLS for crouch gait will vary depending on the patient's physiology, but the major areas of correction are the knee flexors, the knee extensors, and fixed knee contracture.

The knee flexors, primarily the hamstrings, can contribute to crouch gait via their overactivity. If hamstrings are short or spastic they apply excessive force to the knee joint

leading to a higher degree of flexion. To address this issue SEMLS often include a procedure to lengthen the hamstrings or a botox injection to the hamstrings to reduce their activity. These procedures have been shown to have inconsistent results in postoperative studies and can cause complications with the hip joint (Arnold, Liu, Schwartz, Öunpuu, & Delp, 2006). Recent studies have also called into question how great a role spasticity plays in contributing to gait abnormalities (Damiano, Laws, Carmines, & Abel, 2006). In light of this many physicians are moving away from including these procedures in the SEMLS.

The knee extensors, the quadriceps, can contribute to crouch gait via their underactivity. If the quadriceps don't provide enough force, then the leg doesn't fully straighten. The progressively degenerating nature of crouch gait can be explained in part by increasing weakness of the knee extensors. The excessive knee flexion characteristic of crouch gait can cause stretching of the patellar tendon, decreasing the effectiveness of the knee extensors and leading to patella alta, where the patella sits too high in the trochlear groove of the femur. This is counteracted by shortening the lever arm of the patella through a patella tendon advancement (PTA) procedure either by shortening the patellar tendon, moving the attachment site of the patellar tendon, or performing a tibial osteotomy that stretches the patellar tendon (Sossai, Vavken, Brunner, Camathias, Graham, & Rutz, 2015). Shortening of the patellar tendon increases the effectiveness of the quadriceps muscles. While effective in enhancing a patient's ability to achieve full leg extension, care needs to be taken when performing a patellar advancement. Overcorrection can lead to patella baja, where the patella is sitting too low in the

trochlear groove of the femur, which results in higher contact pressures at the patellofemoral joint (Lenhart, Brandon, Smith, Novacheck, Schwartz, & Thelen, 2017).

Fixed knee contracture is a condition often seen in advanced cases of crouch gait where the knee joint is unable to achieve full passive extension, i.e. the leg cannot fully straighten even when the patient is lying down. Fixed knee contracture inherently prevents a patient from achieving full leg extension during gait so whenever the contracture is present a corrective procedure is included in the SEMLS. Two of the most common procedures to correct fixed knee contracture are posterior capsulotomy and distal femoral extension osteotomy (DFEO) (Sossai et al., 2015; Beals, 2007; Healy, Schwartz, Stout, Gage, & Novacheck, 2009). A posterior capsulotomy is usually used to treat mild fixed knee contractures and involves removing a fibrous membrane at the posterior of the knee joint. DFEO is used to treat more severe cases of fixed knee contracture and involves removing a wedge of bone from the supracondylar femur and using plates to reset the bone at a new angle thereby changing the line of action of the leg making it easier to achieve effective full extension.

When deciding on a patient's SEMLS a physician must first determine what factors are contributing to the gait abnormality; overactive knee flexors, weak knee extensors, and/or fixed knee contracture; then decide on procedures to correct each contributing factor. Determining the best possible combination of procedures for treating crouch gait has been the subject of numerous studies. Some trends have emerged but there still isn't an agreed upon gold standard procedure or method to select a procedure. PTA and DFEO have both been shown to have positive postoperative results when included in SEMLS in the short term (Sossai et al., 2015; Healy et al., 2009; Stout et al.,

2008). Long term results are far less studied and are less conclusive, one study showed that in the long-term PTA and DFEO improved stance phase knee extension and knee flexion contracture but showed no improvement in activity or knee pain in early adults (Boyer, Stout, Laine, Gutknecht, Araujo do Oliveira, Munger, ... Novacheck, 2018). A single study comparing the stability of three types of PTA found tibial tubercle osteotomy to be significantly more stable than both imbrication and partial resection and repair at the distal patella (Seidl, Baldini, Krughoff, Shapiro, Lindeque, Rhodes, & Carolo, 2016).

The impact of surgeries on patients is quantified based on a patient's kinematic and/or dynamic data. Kinematic data can be obtained using motion capture technology; reflective markers are attached to anatomical landmarks on the subject and their relative positions used to calculate joint angles and segment lengths. Dynamic data is harder to obtain. At present there exists no method to accurately measure the in vivo forces generated by muscles or the torques created around the joints during subject activity. To get around this inability to accurately measure dynamic data directly, many studies use computer models to simulate subject activity and estimate muscle forces and joint torques. These estimated values can be used to evaluate gait mechanics and identify risk factors thereby providing a metric by which to measure the effectiveness of a procedure.

1.2 Research Goals

The absence of a standardized method for selecting surgical procedures and the lack of a method to provide a quantifiable metrics for the long-term success of a procedure showcases a need for prospective studies to answer the question of how different surgical procedures effect the resulting dynamic forces. This thesis work seeks to address this question by comparing the efficacy of two surgical procedures and

determining the impact of varying surgical parameters on knee joint mechanics and musculoskeletal efficiency. In order to achieve this objective, a computational workflow was developed. The workflow consists primarily of kinematic gait analysis, rigid-body musculoskeletal simulations, and finite element methods. By using computational tools, all variables except the desired independent variable can be held constant between experiments. Changes to the dependent variable can be directly linked to controlled changes. Computational tools also allow for the prediction of parameters that cannot be measured accurately in-vivo—stress and strain in soft tissue and individual muscle forces. Other studies have used models of varying complexity to investigate related topics.

The current state of the art is to use a rigid-body musculoskeletal model to calculate kinematics and muscle forces then use these values in a detailed finite element joint model (Harris, Cyr, Ali, Fitzpatrick, Rullkoetter, Maletsky, & Shelburne, 2016; Lenhart, Brandon et al., 2017; Lenhart, Smith, Schwartz, Novacheck, & Thelen, 2017). Musculoskeletal models have been used to study the kinematics and muscle forces for a variety of gait patterns including crouch gait (Hammer, Seth, Steele, & Delp, 2013; Hoang & Reinbolt, 2012). These studies use rigid musculoskeletal models developed in the program OpenSim in conjunction with motion capture data and ground reaction force data to solve for kinematics and muscle forces examining the changes caused by variations in gait, model constraints, etc. The results of these studies can be validated as much as possible by comparisons with experimentally measured electromyography data on muscle activation. For finite element models the state of the art has recently been moving towards lower limb finite element models with muscle driven kinematics at

certain joints. While not used to study crouch gait several studies have used single leg finite element models with deformable cartilage and muscle driven kinematics (Hume, Navacchia, Rullkoetter, & Shelburne, 2019; Mo, Li, Dan, Liu, & Behr, 2019). These studies have finite element models of a single leg, from foot to pelvis, with rigid bones, deformable cartilage at the knee joint, and varying amounts of soft tissue. The kinematics of the knee joints were dynamically calculated based on muscle forces. In one of these models the muscles were modeled as standard 1D elements with Hill law while in the other they were modeled as 3D elements.

The primary contributions of the research being presented in this thesis are:

- **The development of a computational model capable of estimating dynamic data at the knee joint based on kinematics from the hip, knee and ankle**

This model was applied to estimate the stress and strain on the articular cartilage of the patella based on in vivo kinematics from clinical assessment applied at the hip, ankle, and tibiofemoral joints. Subsequently, proportional-integral feedback control was implemented in this model and used to predict the quadriceps and hamstrings muscle forces required to create appropriate flexion-extension kinematics at the tibiofemoral joint.

- **The evaluation of parametrized effects of varying surgical decisions**

The surgical parameters under investigation were the angle of the bone wedge removed during DFEO and the length of patella tendon shortening during PTA.

The proportional-integral control model described above was used to analyze the

effect of varying the surgical parameters on musculoskeletal requirements while all other variables were held constant.

CHAPTER TWO: MODEL DEVELOPMENT

2.1 Clinical Data Collection

Clinical data was collected by the Children's Hospital Colorado as part of a retrospective study. All participants were patients who had received surgical treatment for cerebral palsy. A total of 11 patients participated ($M = 6$, $F = 5$; surgical age 13.3 ± 1.9 years; $BMI = 18.0 \pm 5.0$). All participants had a primary diagnosis of cerebral palsy, were able to walk unassisted, received surgical treatment including DFEO and/or PTA, and had both pre- and post-operative gait data available. The selected patients showcase a range of crouch gait severity.

Motion capture and force plate data was collected for each patient pre- and post-operatively. A retroreflective marker-based motion capture system was used to record lower limb kinematics at a rate of 120 Hz (Vicon Motion Systems). At the same time ground reaction forces and moments were recorded at 1080 Hz by in-ground force plates. A fourth-order zero-lag low-pass Butterworth filter was used to filter out random noise, the cutoff frequency used was 40 Hz (Yu, Gabriel, Noble, & An, 1999). The placement of retroreflective markers followed a published protocol from the literature (Davis III, Ounpuu, Tyburski, & Gage, 1991). Data from a standing trial was taken to be used for marker calibration and patient specific scaling factors. The subsequent gait trial was conducted with the patients walking at a self-selected pace. Data was collected for each patient pre-operatively then again after each patient underwent surgical treatment for crouch gait. As part of a typical clinical referral the gait laboratory findings were

analyzed to provide surgical recommendations to the attending physician who ultimately selects the surgical procedures included in the SEMLS (Chang, Seidl, Muthusamy, Meininger, & Carollo, 2006).

2.2 Rigid-Body Musculoskeletal Model

The open source software OpenSim is used to develop rigid-body musculoskeletal models and create dynamic simulations (Delp, Anderson, Arnold, Loan, Habib, John, & Thelen, 2007). These simulations can predict muscle forces which cannot be measured in vivo using non-intrusive means. The model used in this research is a previously developed lower limb and torso model; it has 14 bony bodies, 92 musculotendon units, 23 degrees of freedom, 19 of which are active, and 19 markers (Navacchia, Myers, Rullkoetter, & Shelburne, 2016).

Each patient's standing trial was used to calibrate marker locations and determine patient specific scaling factors. Each marker from a patient's motion capture was matched to the corresponding marker of the musculoskeletal model. Then scaling factors and kinematics of the musculoskeletal model were adjusted to best match the locations of the patient's marker data. Greater weight was given to markers with higher degrees of placement accuracy; for instance, markers placed on bony prominences like the iliac crest were given a higher weighting than those placed on soft tissue like the thigh. A total of five scaling factors were calculated for each model: anterior-posterior (AP), medial-lateral (ML), and three distal-proximal (DP) parameters. The AP and ML factors were based on markers on the pelvis and were applied evenly to the entire model. The DP factors were based on different body segments and applied to specific body segments. The first factor was based on the thigh using markers from the hip and knee. This factor

was applied to the femur and patella. The second factor was based on the shank using markers from the knee and ankle and was applied to the tibia and fibula. The final factor was based on the entire lower torso using markers from the pelvis and heel and was applied to all other bones. All 3 DP scale factors were averaged across the left and right legs.

The marker pairings and scaling factors found in the standing trial were applied in the gait trial (Figure 1). The motion capture and ground-reaction forces of the gait trial were used as inputs to create a dynamic simulation capable of predicting the required muscle forces. Individual muscle forces were estimated using a static optimization technique that solves equations of motion while minimizing the sum of squared muscle activations at each time step (Anderson & Pandy, 2001). To facilitate inter-subject comparison and account for varying walking stride and speed between patients, kinematic and force data from a single gait cycle was extracted for each subject and normalized so that 0 and 100% were sequential heel strikes.

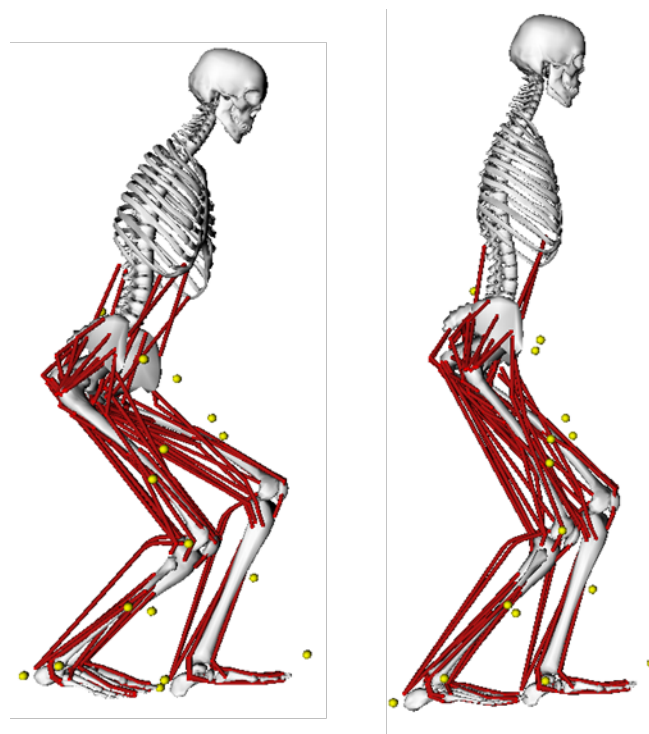


Figure 1 Pre- (left) and post- (right) operative rigid-body musculoskeletal model in OpenSim during gait cycle simulation

2.3 Kinematics

Kinematics for the left and right hip, tibiofemoral, and ankle joints were calculated using the patient's motion capture data. The data is used to create a series of transformation matrices that describe the relative position of each body segment, left femur, right talus, etc. during every frame of the gait cycle. Kinematics were calculated based on the clinical axes; ML, AP, and DP with each axis having both translation and rotation for a total of six degrees of freedom (Grood & Suntay, 1983). Each joint has its own coordinate system based on these clinical axes. The joint coordinate system is in turn based on the local coordinate systems of the two bones that create the joint. A local coordinate system was created for every bone involved in a joint. Physicians define clinical axes based on bony landmarks. The DP axis of the femur is defined as passing through the center of the femoral head and the most distal point of the posterior surface

halfway between the medial and lateral condyles. Other axes are defined similarly. To define these axes in the model nodes were selected from the bone's geometry that most closely matched the bony landmarks used by physicians (Figure 2).

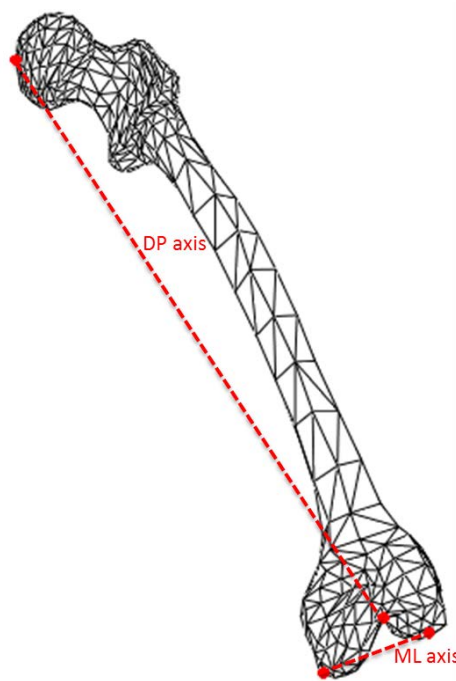


Figure 2 Left femur geometry with DP and ML axes and the nodes used to create said axes

The coordinate systems of the joints were created based on the bone coordinate systems. The DP axis of the joint is identical to the DP axis of one bone and the ML axis of the second bone is the ML axis of the joint. The AP axis of the joint is the cross product of the joint's DP and ML axes (Figure 3). This creates a joint coordinate system where the DP axis and ML axis are each based on a different bone and the joint AP axis is perpendicular to both the DP and ML axes (Figure 4).

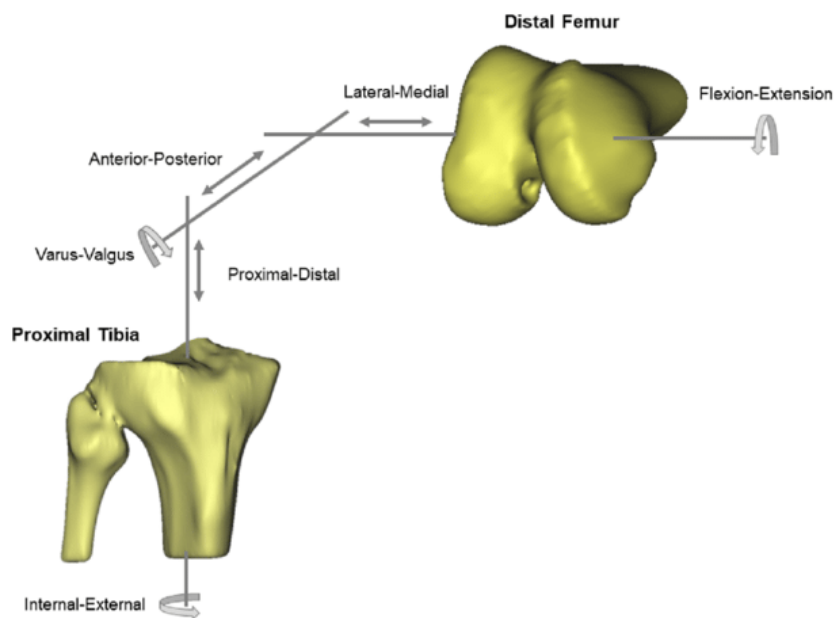


Figure 3 Exploded view of tibiofemoral joint coordinate system axes (Naendrup, Zlotnicki, Murphy, Patel, Debski, & Musahl, 2019)

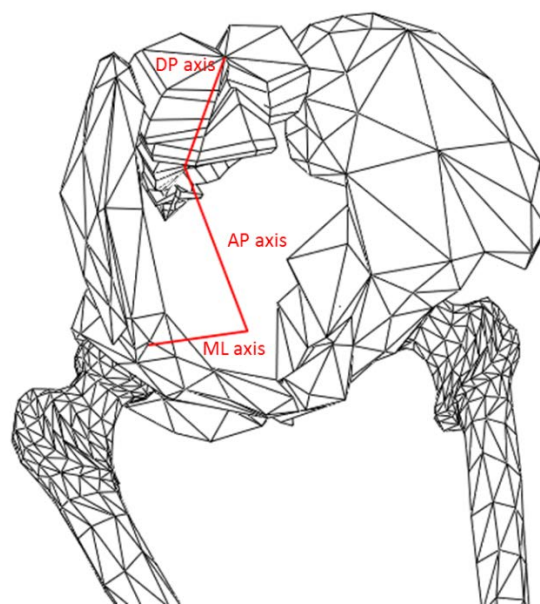


Figure 4 Right hip joint coordinate system axes

These joint axes are used in conjunction with the origin of the superior bone to create a transformation matrix that describes how the coordinate system of the superior bone relates to that of the inferior bone. Grood and Suntay developed a series of equations that can be used to calculate the joint kinematics from these transformation

matrices (Grood & Suntay, 1983). The equations are effective for the most part but required two improvements to be usable for this study. Firstly, the equation to calculate translation along the ML axis fails to account for the effective translation that results from rotation along the AP axis. An additional component of the equation was added to calculate this incidental translation and remove it from the calculated ML translation. The second improvement was more minor. When calculating the flexion-extension angle, rotation around the ML axis, the function atan2 is used instead of the basic atan. Without this change the angle can be calculated to be in an incorrect quadrant causing a discontinuity in the kinematics. This comes into play when the flexion-extension angle changes from positive to negative so it is not generally necessary for the tibiofemoral joint but is necessary for the hip and ankle.

2.4 Knee Finite Element Model

A detailed finite element model of the left and right knee joints, tibiofemoral and patellofemoral, was created. The model includes rigid bones, deformable articular cartilage, and spring-based ligaments and tendons. 3D knee imaging was not a component of the gait analysis performed on the involved patients and so it was not possible to create patient specific models. Instead imaging data of a non-pathological knee from a publicly available repository was used (Harris et al., 2016). The commercial software Amira was used create and align segmented geometries; bone geometries were extracted from computed tomography scans and articular cartilage geometries were extracted from magnetic resonance scans (ZIB, Berlin, Germany). Medial and lateral patellofemoral ligaments, patellar tendon, and rectus femoris and vasti tendons were modeled as 2D fiber-reinforced membranes and aligned with the segmented bone

geometries based on bony prominences. The fibers were represented as tension-only non-linear springs, as is consistent with other models used in the literature (Fitzpatrick, Baldwin, Ali, Laz, & Rullkoetter, 2011). The entire model was scaled for each patient using the ML, AP, and thigh DP scaling factors calculated with the musculoskeletal model.

2.5 Lower Extremity Finite Element Model

The final model used in the research is a finite element model which combines both the musculoskeletal and finite element models described in sections 2.2 and 2.4 to create a comprehensive finite element model of the lower limb and associated musculature. First, the musculoskeletal model was converted into a finite element model. The transformation matrices, from section 2.3, of the first frame of the gait cycle can be used to convert the geometries of the musculoskeletal model to the coordinate system of a finite element model. This was used to find the coordinates of the bones and muscles of interest for the final model. The pelvis and bones of the lower limbs were included. The muscles of interest were the four quadriceps bundles—rectus femoris, vastus lateralis, vastus medialis, and vastus intermedius—and the four hamstrings bundles—semitendinosus, semimembranosus, and both the long and short head biceps femoris. The same kinematic axes used in the musculoskeletal model described in section 2.3 were reproduced in the finite element model. To do this, a node set was created that included the nodes at bony landmarks used to create the kinematic axes and nodes at the calculated locations for the AP axis. The axes themselves were created as 3D connector elements between the two appropriate nodes.

The new finite element version of the musculoskeletal model and the knee finite element model were combined into the final model by aligning the femurs and tibias of each component. The femurs are aligned first using a best fit of the three clinical axes of the femur, ML, AP, DP. Once the femurs are aligned, the tibia of the knee model, which is initially positioned in full extension, is flexed into position with the tibia extracted from the musculoskeletal model based on the initial gait kinematic values. The initial gait muscle forces are also applied, pulling the patella into position (Figure 5).



Figure 5 Sagittal (left), frontal (middle), and angled (right) view of lower extremity finite element model

2.6 Proportional-Integral Controlled Muscles

Proportional-integral control of the muscles is achieved through integration of a FORTRAN-based user subroutine within Abaqus, a finite element software. The control system, coded in FORTRAN, run simultaneously with Abaqus's finite element solver and

it reads in both the desired target flexion profile and the model's current flexion then adjusts the forces applied by the muscles in the model in order to match the model profile with the target profile. The control system measures the difference between the actual and target flexion and either increases or decreases a muscle's force accordingly. The magnitude of the muscle force is changed is based on two metrics. The first is the instantaneous difference between target and actual flexion, the second metric is based on a running integral of the difference between target and actual flexion profiles. Each metric was weighted to determine how much it influenced the changed level of muscle force. The weights for each model were calibrated in an effort to minimize the root mean square error between the desired and actual flexion profiles (Figure 6).

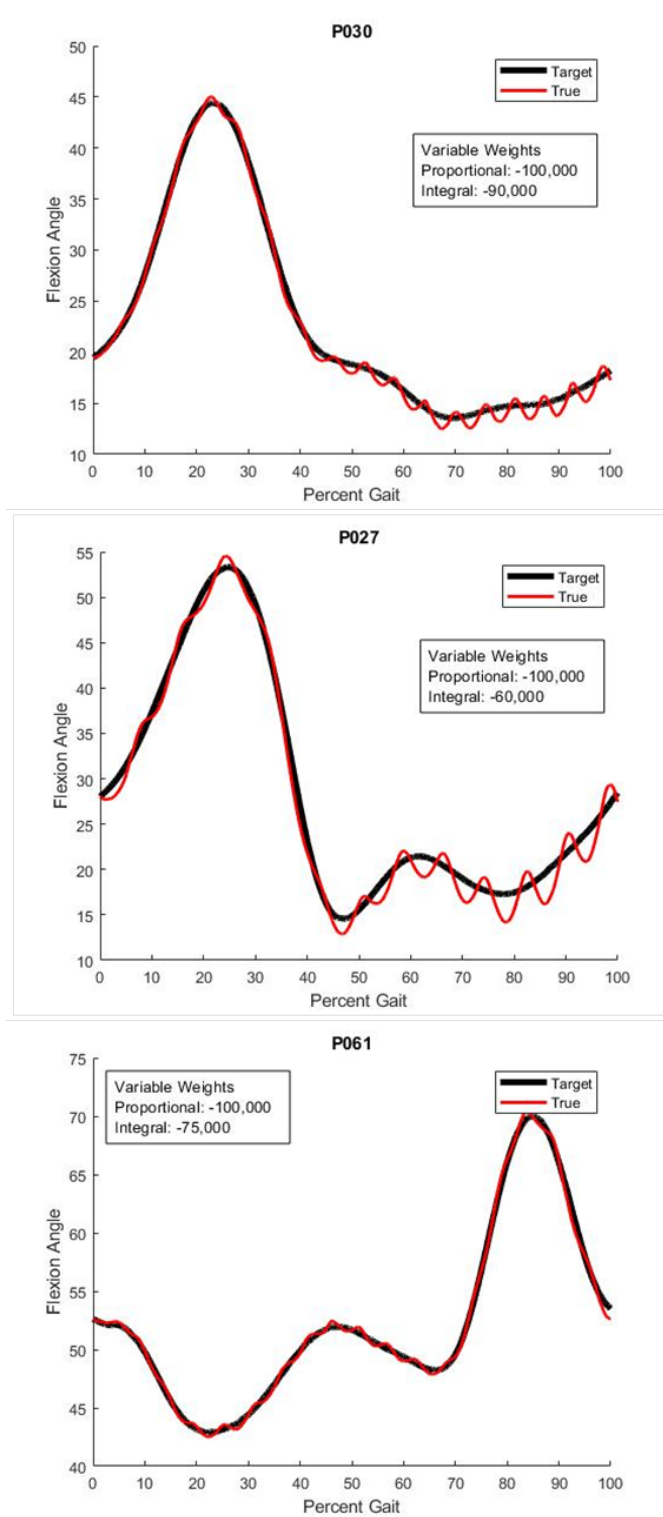


Figure 6 Comparison of target and achieved tibiofemoral flexion-extension angle for three patients

2.7 Model Application

In this work, the model development described above was implemented to investigate the efficacy of differing surgical procedures used to treat crouch gait. A lower extremity finite element model using the muscle forces calculated with the rigid-body musculoskeletal model was used to study the effects of the surgeries. The models were modified to include the surgical procedures used on the patients and the conditions of the patellar articular cartilage were compared between models. Comparisons were made between pre- and post-operative models as well as between models that included different surgical procedures. An additional model was developed using the proportional-integral control system. Multiple simulations were run with the same model modified to have different surgical procedures. The calculated muscle forces were compared between the models of different surgeries. This is described in detail in Chapters 3 and 4.

CHAPTER THREE: MANUSCRIPT “EFFECT OF CORRECTIVE SURGERY ON LOWER LIMB MECHANICS IN PATIENTS WITH CROUCH GAIT”

3.1 Introduction

Cerebral palsy is a neurological disorder found in roughly 0.36% of children in the US (Yeargin-Allsopp et al., 2008). Crouch gait is one of the most common gait deviations found in patients with cerebral palsy (Rethlefsen et al., 2016). Crouch gait is characterized by an excessive amount of flexion at the knee joint during gait. It is a progressively degrading gait deviation; in part because the crouched posture itself reduces the capacity for muscles to generate extension accelerations at the hip and knee joints (Hicks et al., 2008).

Over time a patient’s gait can decay to the point where they are non-ambulatory and require assistive devices such as a walker or wheelchair to move around. Current treatment for these advanced stages of crouch gait involves surgical intervention. Single event multi-level surgery (SEMLS) has been accepted as the preferred method to treat musculoskeletal deformities and gait deviations in patients with cerebral palsy and has been proven to provide both short- and long-term improvement (Lamberts et al., 2016; Öunpuu et al., 2015). The surgical procedures included in the SEMLS for crouch gait will vary depending on the patient’s physiology, but the major areas of correction are the knee flexors, the knee extensors, and fixed knee contracture.

The knee flexors, primarily the hamstrings, can contribute to crouch gait via their over activity. If hamstrings are short or spastic they apply excessive force to the knee

joint leading to a higher degree of flexion. To address this issue SEMLS often include a procedure to lengthen the hamstrings or a botox injection to the hamstrings to reduce their activity. These procedures have been shown to have inconsistent results in postoperative studies and can cause complications with the hip joint (Arnold et al., 2006). Recent studies have also called into question how great a role spasticity plays in contributing to gait abnormalities (Damiano et al., 2006). In light of this many physicians are moving away from including these procedures in the SEMLS.

The knee extensors, the quadriceps, can contribute to crouch gait via their underactivity. If the quadriceps don't provide enough force, then the leg doesn't fully straighten. The progressively degenerating nature of crouch gait can be explained in part by increasing weakness of the knee extensors. The excessive knee flexion characteristic of crouch gait can cause stretching of patellar tendon decreasing the effectiveness of the knee extensors and leading to patella alta—the patella sitting too high in the trochlear groove of the femur. This is counteracted by shortening the lever arm of the patella through a patella tendon advancement (PTA) procedure either shortening the patellar tendon, moving the attachment site of the patellar tendon, or performing a tibial osteotomy that stretches the patellar tendon (Sossai et al., 2015). The effective shortening of the patellar tendon increases the effectiveness of the quadriceps muscles. While effective in enhancing a patient's ability to achieve full leg extension, care needs to be taken when performing a patellar advancement. Overcorrection can lead to patella baja, the patella sitting too low in the trochlear groove of the femur, which results in higher contact pressures at the patellofemoral joint (Lenhart, Brandon et al., 2017).

Fixed knee contracture is a condition often seen in advanced cases of crouch gait where the knee joint is unable to achieve full passive extension, i.e. the leg cannot fully straighten even when the patient is lying down. Fixed knee contracture inherently prevents a patient from achieving full leg extension during gait so whenever the contracture is present a corrective procedure is included in the SEMLS. Two of the most common procedures to correct fixed knee contracture are posterior capsulotomy and distal femoral extension osteotomy (DFEO) (Sossai et al., 2015; Beals et al., 2007; Healy et al., 2009). A posterior capsulotomy is usually used to treat milder fixed knee contractures and involves removing a fibrous membrane at the posterior of the knee joint. DFEO is used to treat more severe cases of fixed knee contracture and involves removing a wedge of bone from the supracondylar femur and using plates to reset the bone at a new angle thereby changing the line of action of the leg making it easier to achieve effective full extension.

When deciding on a patient's SEMLS a physician must first determine what factors are contributing to the gait abnormality; overactive knee flexors, weak knee extensors, and/or fixed knee contracture; then decide on procedures to correct each contributing factor. Determining the best possible combination of procedures for treating crouch gait has been the subject of numerous studies. Some trends have emerged but there still isn't an agreed upon gold standard procedure or method to select a procedure. PTA and DFEO have both been shown to have positive postoperative results when included in SEMLS in the short term (Sossai et al., 2015; Healy et al., 2009; Stout, Gage, Schwartz, & Novacheck, 2008). Long term results are far less studied and are less conclusive, one study showed that in the long-term, PTA and DFEO improved stance

phase knee extension and knee flexion contracture but showed no improvement in activity or knee pain in early adults (Boyer et al., 2018). A single study comparing the stability of three types of PTA found tibial tubercle osteotomy to be significantly more stable than both imbrication and partial resection and repair at the distal patella (Seidl et al., 2016).

The impact of surgeries on patients is quantified based on a patient's kinematic and/or dynamic data. Kinematic data can be obtained using motion capture technology; reflective markers are attached to anatomical landmarks on the subject and their relative positions used to calculate joint angles and segment lengths. Dynamic data is harder to obtain. At present there exists no method to accurately measure the forces generated by muscles or the torques created around the joints during subject activity. To get around this inability to accurately measure dynamic data, many studies use computer models to simulate subject activity and estimate muscle forces and joint torques. These estimated values can be used to evaluate gait mechanics and identify risk factors thereby providing a metric by which to measure the effectiveness of a procedure.

The objective of this work is to develop a computational model capable of estimating dynamic data at the knee joint based on kinematics from the hip, knee and ankle. The model will include left and right hip, tibiofemoral, patellofemoral, and ankle joints each with 6 DOF. The kinematics of the patellofemoral joint will be determined by the finite element solver based on the kinematics of the other joints, muscle forces, and stabilizing forces from tension resistant ligaments. Patient data will be used with the model to simulate the patient's gait. Adjustments to the model will be made to reflect the corrective surgeries, DFEO and/or PTA, include in the patient's SEMLS. The condition

of the patella's articular cartilage will be compared across models to study the efficacy of the two surgeries.

3.2 Methods

The Children's Hospital Colorado has provided motion capture and force plate data from 11 patients who have a primary diagnosis of crouch gait and received treatment that included a SEMLS with a PTA and/or DFEO procedure. Each patient had data collected both before surgical treatment and after recovering from surgery. Collected data included both a gait trial and a static trial.

A finite element model has been developed based on the provided patient data supplemented with an available musculoskeletal model and magnetic resonance images and computed tomography scans from a freely available database. Kinematic data, both pre- and postoperative, were obtained from 11 patients who underwent PTA and/or DFEO procedures to correct for crouch gait. A 3D finite element model of the lower extremity (including bone, cartilage, extensor mechanism, soft-tissue, muscle) was developed in Abaqus/Explicit (Figure 7). Detailed, deformable representations were included at the knee joint (Figure 7).

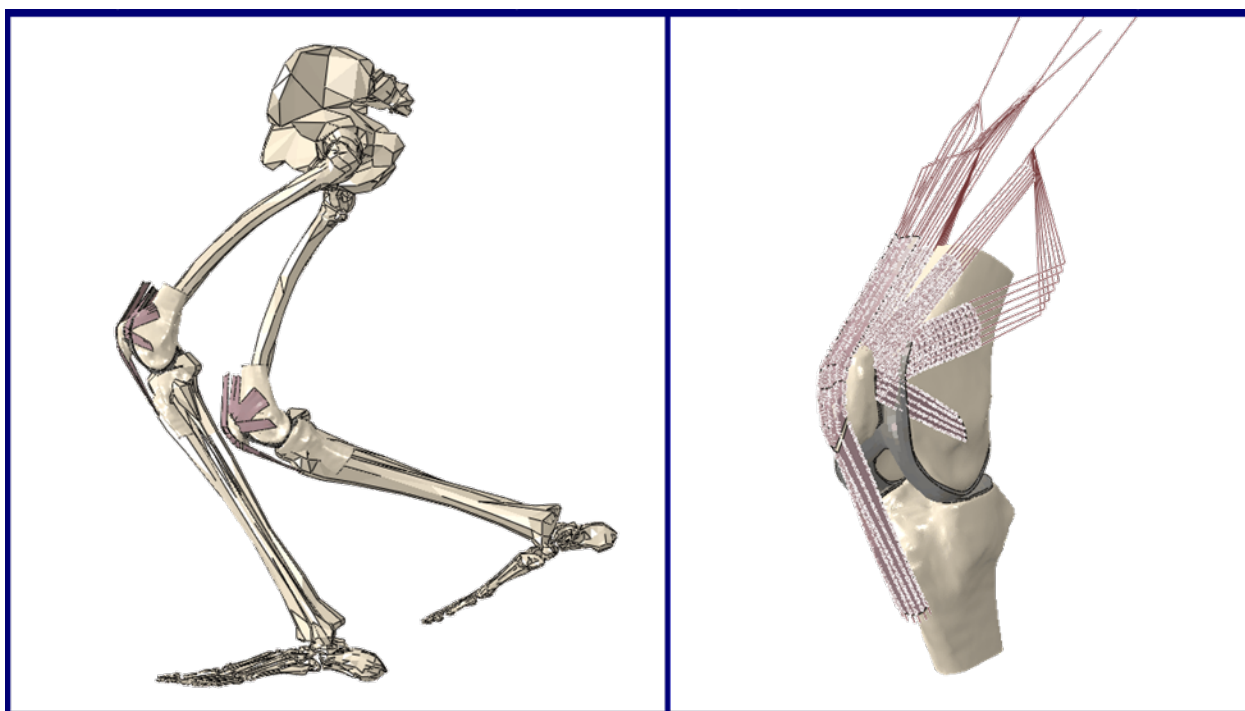


Figure 7 Finite element model: combined model (left) and detailed knee (right)

The second component of the final model was a more detailed model of the patellofemoral and tibiofemoral joints which includes rigid bone, deformable cartilage, tendons, and ligaments. The more detailed model included rigid bone for the patella and the heads of the femur and tibia; deformable articular cartilage on the patella, femur, and tibia; spring based medial patellofemoral ligament, lateral patellofemoral ligament, patella tendon, and tendons for the four quadriceps. The geometry of the more detailed bones was based on freely available CT scans of a nonpathological knee. MRI scans from the same freely available data set was used to create the geometry of the articular cartilage. The geometries of bone and cartilage were reconstructed and combined using the commercial software, Amira (FEI, OR) then meshed using Hypermesh (Altair, MI). The attachment sites for the tendons and ligaments are based on bony prominences. The bones were modeled as rigid bodies, the cartilage as eight-noded isoparametric elements with reduced integration, and the ligaments and tendons as a combination of 2D elements

and springs. The properties of all the non-rigid elements were based on experimental values used in a previously validated finite element model.

The two components were combined into the final model by aligning the femurs and tibias of each component. The femurs are aligned first using a best fit of the three clinical axes of the femur, ML, DP, and AP. Once the femurs are aligned, the tibia of the detailed knee model, which is initially positioned in full extension, is flexed into position with the tibia extracted from the OpenSim model based on the initial gait kinematic values. The initial gait muscle forces are also applied, pulling the patella into position.

Inverse kinematics and dynamics were used to derive joint mechanics and muscle forces for gait analysis. The rigid-body musculoskeletal modeling software OpenSim, used to create the first component, was used to perform these calculations based on a Vicon lower extremity marker-based motion capture system and in-ground force plates. The coordinate system developed by Grood and Suntay was used to calculate the kinematics of the hip, tibiofemoral, and ankle joints of both the left and right legs (Grood & Suntay, 1983). Joint moments were calculated using the in-built inverse dynamics tool in OpenSim based on the kinematics data and the ground reaction force plate data. Individual muscle forces were estimated using a static optimization technique that solves equations of motion while minimizing the sum of squared muscle activations at each time step (Anderson & Pandy, 2001).

Each model was scaled with patient specific values based on the motion capture data from the patient's static trial. A total of five scaling factors were calculated for each model: anterior-posterior, medial-lateral, and three distal-proximal parameters. The anterior-posterior and medial-lateral factors were based on markers on the pelvis and

were applied evenly to the entire model. The distal-proximal factors were based on different body segments and applied to specific body segments. The first factor was based on the thigh using markers from the hip and knee. This factor was applied to the femur, patella, tendons, and ligaments. The second factor was based on the shank using markers from the knee and ankle and was applied to the tibia and fibula. The final factor was based on the entire lower torso using markers from the pelvis and heel and was applied to all other bones. All three distal-proximal scale factors were averaged across the left and right legs.

The final finite element model was modified to represent pre- and postoperative conditions. The pre-operative model was modified to represent the pathological preoperative condition by lengthening the patella tendon (Figure 8). Patient-specific information about the PTA procedure didn't include the amount by which the patella tendon was shortened from its preoperative condition, so all models used a consistent value of 2 cm. The postoperative model was modified by rotating the more detailed femur bone about its medial-lateral axis to mimic the DFEO. Radiographs were included for some patients, pre- and/or postoperative. When a postoperative radiograph was included for a patient who's SEMLS included DFEO, then an edge finding function in MATLAB was used to find the angle between the femur head and the main length of the femur (Figure 9). If no post-surgery radiograph was provided then a 30° rotation was used for the baseline model. This angle was typical of a DFEO surgery for severe crouch gait (Lenhart, Smith et al., 2017). The patients in this study were selected to showcase a

range of crouch severity. Of the available radiographs showing DFEO, almost half (3 of 7) showed an angle of $30^{\circ} \pm 2^{\circ}$ while the remaining showed an angle of less than 15° .

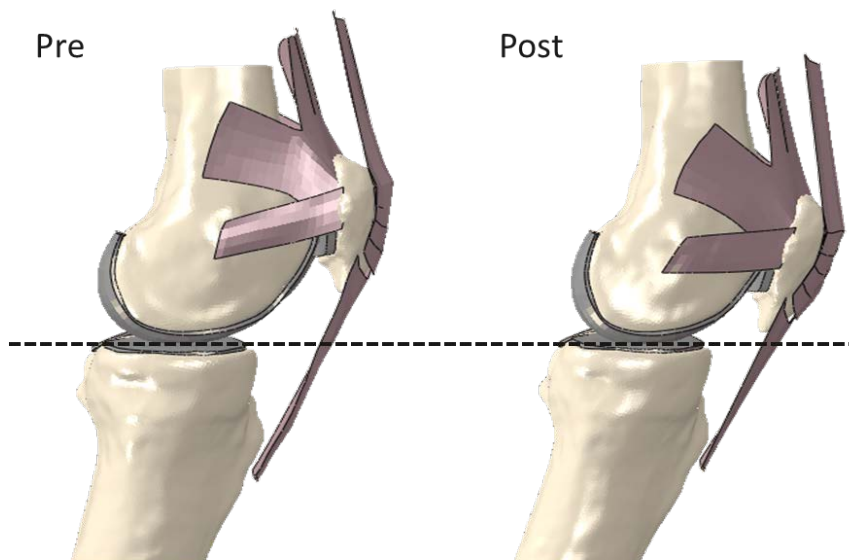


Figure 8 Detailed knee finite element model used for patients treated with PTA pre-surgery (left) and post-surgery (right)

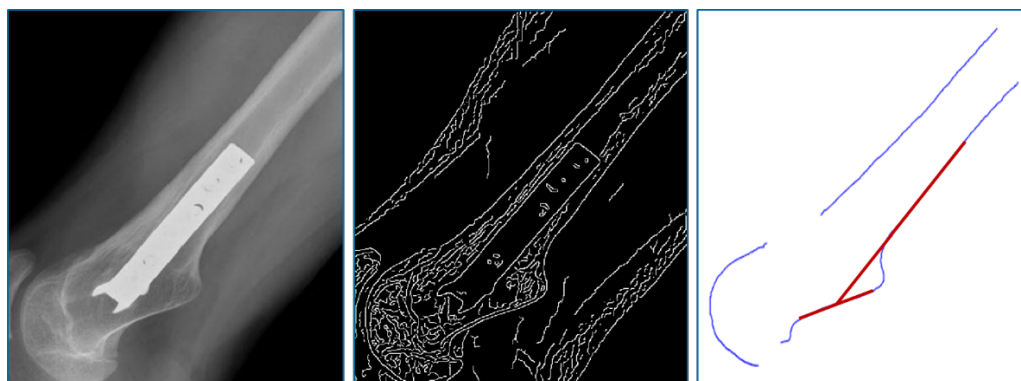


Figure 9 X-ray (left), edge detection (middle), and lines for angle calculation (right)

Each model was run for a single gait cycle in the finite element solver Abaqus to solve for the contact mechanics at the patellofemoral joint. The kinematics for the hip, tibiofemoral, and ankle joints as well as the muscle forces of the quadriceps are based on the values calculated by OpenSim. The 6-DOF pose of the patellofemoral joint was

kinematically unconstrained and was determined based on applied forces and contact mechanics. The quadriceps apply force to the patella through their respective tendons, while the patella tendon and patellofemoral ligaments provide a spring-based resistive force. Geometric constraint was enabled by defining contact between the articular cartilage of the femur and patella. The primary variables of interest were stress, both average and maximum, and contact area. Higher stress values or more concentrated stress, indicated by a smaller contact area, indicate a higher risk for a patient to develop early onset osteoarthritis.

The mean and standard deviation of the 90th percentile von mises stress, contact area between the patellar and femoral articular cartilage, and the tibiofemoral flexion-extension kinematics were extracted from the models. The 90th percentile of the von mises stress was chosen for comparison instead of the maximum value to prevent a singular element with excessive stress, a possible result of hourglassing in finite element models, from effecting the data. Data was collected from both the left and right knee of each model but models varied in which leg's heel strike began the gait cycle. To facilitate comparisons the data was categorized as belonging to either the leading leg, the leg whose heel strike begins the gait cycle, or the lagging leg. Comparisons between the pre- and post-operative results as well as between the knees that had undergone both DFEO and PTA and those that only had PTA were assessed using a Wilcoxon rank sum test with significance determined at $p \leq 0.05$.

3.3 Results

When comparing the pre- and post-operative knees, all metrics had instances of significant difference. The flexion-extension kinematics showed consistently higher

degrees of flexion pre-operatively (Figure 10). Von mises stress and contact area between patellar and femoral articular cartilage each had several instances where pre-operative values were higher than post-operative (Figure 11 and 12). A single patient's contact stress map also shows higher concentrations of stress pre-operatively with the highest concentration near the edge of the articular cartilage which increases the risk of cartilage wear and early onset osteoarthritis (Figure 13).

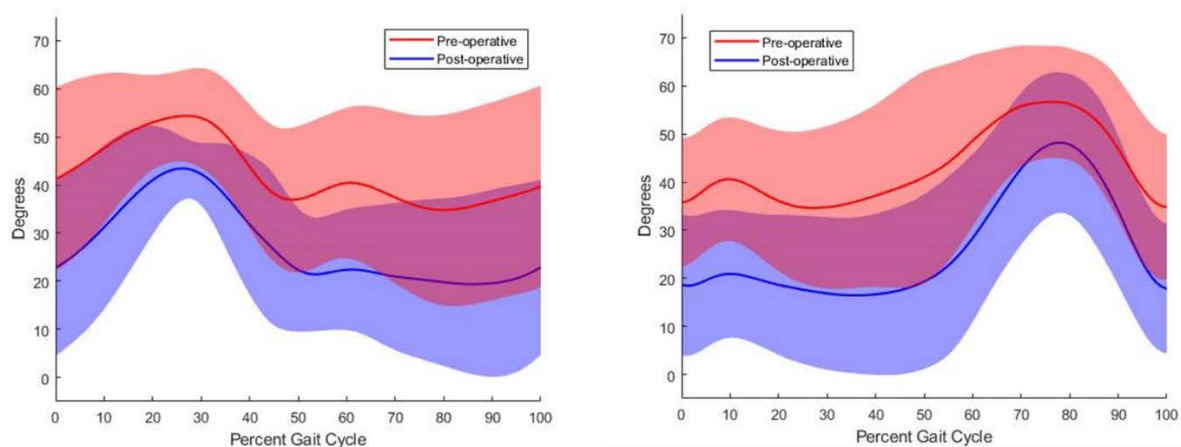


Figure 10 Tibiofemoral flexion-extension kinematics pre- and post-operative; lagging leg (left) and leading leg (right)

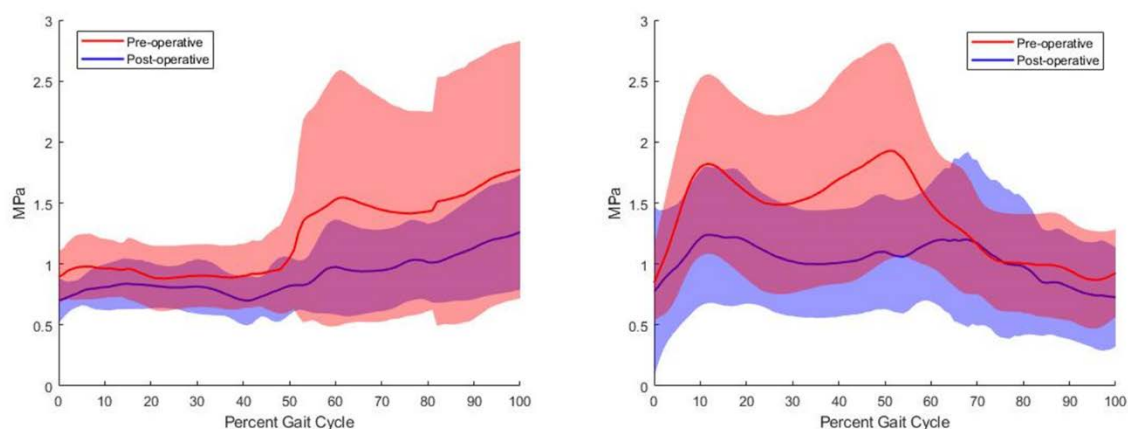


Figure 11 90th percentile von mises stress pre- and post-operative; lagging leg (left) and leading leg (right)

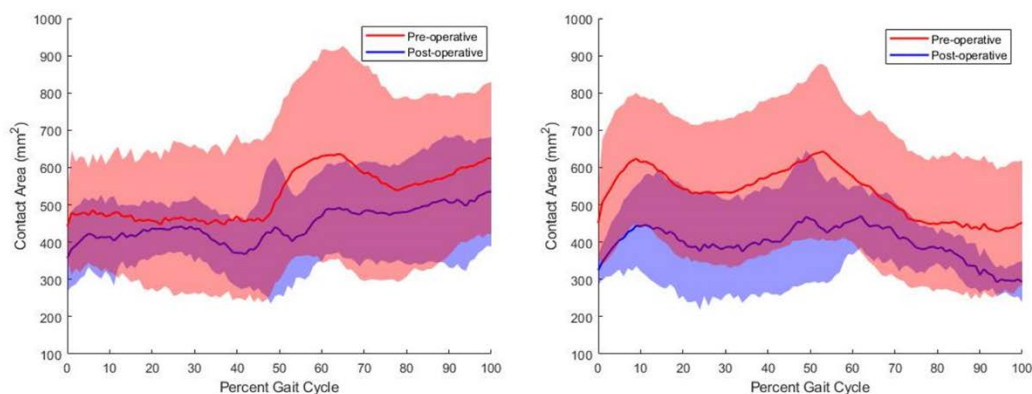


Figure 12 Contact area of patellar articular cartilage pre- and post-operative; lagging leg (left) and leading leg (right)

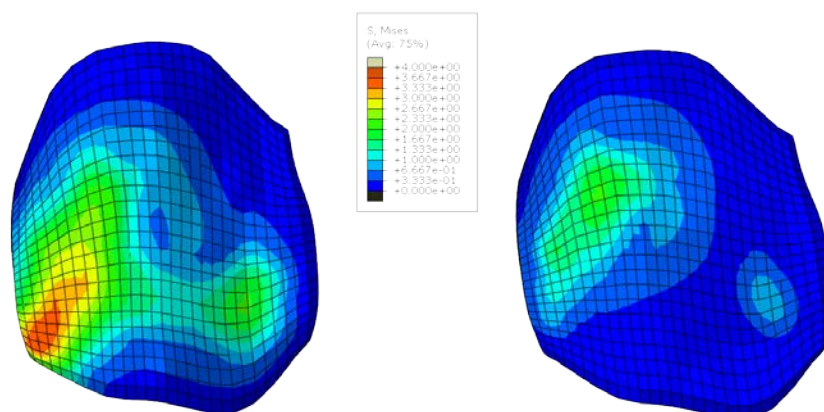


Figure 13 Stress on patellar articular cartilage of same patient pre- (Left) and post-operatively (Right)

Comparisons between post-operative models with both DFEO and PTA and those with only PTA found significant differences in contact area, with DFEO and PTA model data having higher values. The only significant difference found between pre-operative models was tibiofemoral flexion-extension, with the models including both DFEO and PTA having higher extension values (Figure 14).

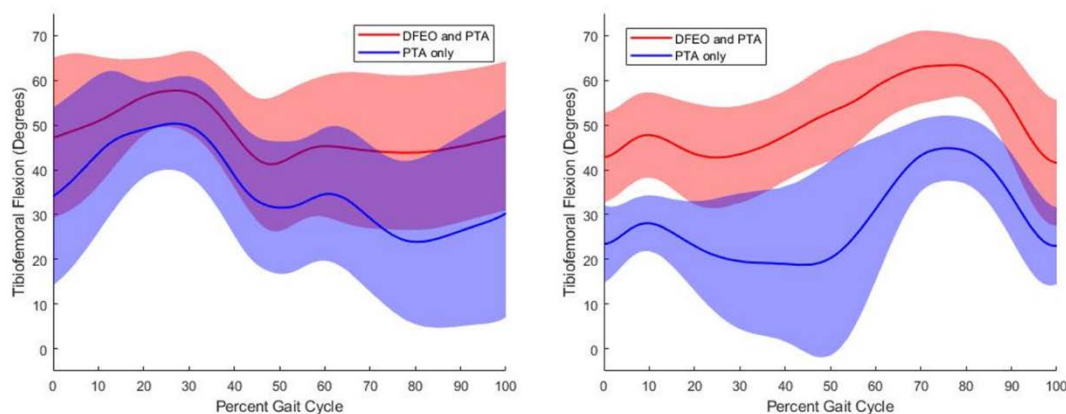


Figure 14 Tibiofemoral flexion-extension kinematics pre-operative; lagging leg (left) and leading leg (right)

3.4 Discussion

The goal of this project is to quantitatively evaluate the effect of corrective surgeries on patellofemoral joint mechanics in patients with crouch gait. By comparing the efficacy of different surgeries, recommendations can be made as to which procedures physicians should select when developing a treatment plan. The differences in the tibiofemoral flexion-extension kinematics between the pre- and post-operative models show that the surgeries were successful in creating gait kinematics with reduced flexion angles. The higher flexion in the pre-operative models with DFEO and PTA paired with the lack of significant difference between post-operative models with different surgeries indicates that including a DFEO in a patient's SEMLS gives a patient with a worse diagnosis the same post-operative outcome, in terms of gait kinematics, as a patient with a milder diagnosis. The higher contact area seen in the post-operative models that included both DFEO and PTA suggests that the combination of surgical procedures may lead to more dispersed stress on the patellar articular cartilage which would reduce wear.

The higher von mises stress in the post-operative model indicate that the surgeries are successful at lowering a patient's chance of early-onset osteoarthritis however this

may be mitigated by the lowered contact area. It depends in part on where the stress is concentrated on the patellar articular cartilage and how much the decreased contact area is the result of decreased stress. The edges of the patellar articular cartilage are more vulnerable to wear. The stress concentration map in Figure 13 shows that while the pre-operative von mises stress is spread out over more of the cartilage the area of highest stress is at the edge of the cartilage increasing the risk of wear.

Future work should be done to fully validate the developed model. The soft tissue properties and set up of the knee joint finite element model were based on a previously published patellofemoral model that had kinematic agreement with existing literature and had patellofemoral contact mechanics validated with experimental pressure-sensitive film data (Fitzpatrick et al. 2011). In order to validate the full lower torso finite element model cadaveric studies could be done to simulate gait and deep knee bend activities. Strain and stress could be measured experimentally using strain sensors and pressure-sensitive film and used to valid the dynamics and contact mechanics of the corresponding computational model.

The procedure developed in this study to quantify the effects of corrective surgery on lower limb joint mechanics based on patient motion capture and force plate data can be used for further study with additional patient groups. The effectiveness of different corrective procedures could be investigated, as well as the impact of different patient specific characteristics. In this study the procedures included in the model were a direct match to the procedure ultimately selected for the patient, a further study could instead focus on performing different procedures on a single model to more directly compare the outcomes of those surgeries.

CHAPTER FOUR: PROPORTIONAL INTEGRAL FEEDBACK CONTROL AND THE PARAMETRIC ASSESSMENT OF SURGICAL DECISIONS

4.1 Introduction

The differences between patients SEMLS are dependent on more than just surgery selection. Many surgical procedures have factors that vary depending on the patient's particular physiology. These surgical decisions can have an outcome on the patient's final condition. During PTA, the attending surgeon shortens the tendon by a length equal to the tendon's width (Novacheck, Stout, Gage, & Schwartz, 2009). The angle of the bone wedge removed in DFEO is determined by the surgeon intraoperatively. The proximal line of the wedge is created so that it is perpendicular to the line of the tibia, measured using an orientation plate during surgery. The distal line of the wedge starts at the same point on the posterior of the bone but is perpendicular to the femur (Plexus Surgical Video Productions).

The muscle force needed to achieve a target kinematic profile can be an effective means of judging the effectiveness of a surgical procedure. Lowering the required muscle force makes the target kinematic profile easier for the patient to achieve. The objective of this study was to develop a computational model capable of comparing the muscle forces needed to achieve the same kinematics after being modified to mimic varying surgical procedures.

4.2 Methods

The model described in Section 3.2 was modified to include a proportional-integral feedback control system for the muscles that was used to calculate flexion-extension motion of the tibiofemoral joint. By developing a subroutine to solve for both muscle forces and tibiofemoral flexion-extension based on a desired flexion profile we introduce muscle forces as a dependent creating more metrics by which we may judge the efficacy of differing surgical procedures. Having tibiofemoral flexion-extension muscle driven instead of directly prescribed also allows for contact between the articular cartilage of the tibia and femur. While not a focus of this study having a model capable of calculating inter-joint mechanics such as stress at the tibiofemoral joint will be beneficial to future work. Proportional-integral control of the muscles is achieved through a combination of Abaqus and FORTRAN. The control system coded in FORTRAN run simultaneously with Abaqus's finite element solver and it reads in both the desired flexion profile and the model's current flexion then adjusts the muscle forces in the model to best achieve the desired flexion. The control system measures the difference between the actual and desired flexion and either increases or decreases a muscles activation accordingly. How much the activation is changed is based on two components. The first is the instantaneous difference between desired and actual flexion, the second component is based on a running integral of the difference between flexions. Each component was weighted to determine how much it influenced the changed level of muscle activation. The weights for each model were calibrated in an effort to minimize the root mean square error between the desired and actual flexion profiles.

The final model was modified to study the effect of two different surgical procedures and their associated surgical decision. The patient data provided for this study was collected by the Children's Hospital Colorado. Each patient was treated for a primary diagnosis of crouch gait, treatment included a SEMLS with a PTA and/or DFEO procedure. The baseline model for each patient was modified to include the appropriate procedures. Additional models were created to include a single surgical procedure with varying surgical decisions. For the PTA procedure all baseline models used a patella tendon of healthy length, surgical decision models have patella tendons of varying lengths (Figure 15). For the DFEO procedure the detailed femur head was rotated about its ML axis to simulate the change in bone shape achieved by the surgery. Some patients had SEMLS that did not include a DFEO, for these patients the baseline model had no rotation. If a post-surgery radiograph was included for the remaining patients, the angle of rotation was determined using edge detection software to find the angle between the femoral head and shaft (Figure 16). If no post-surgery radiograph was provided, a 30° angle of rotation was used for the baseline model. This angle was typical of a DFEO surgery for severe crouch gait (Lenhart, Smith et al., 2017). Surgical decision models were created for each patient with DFEO rotations of 0, 15, and 30 degrees.

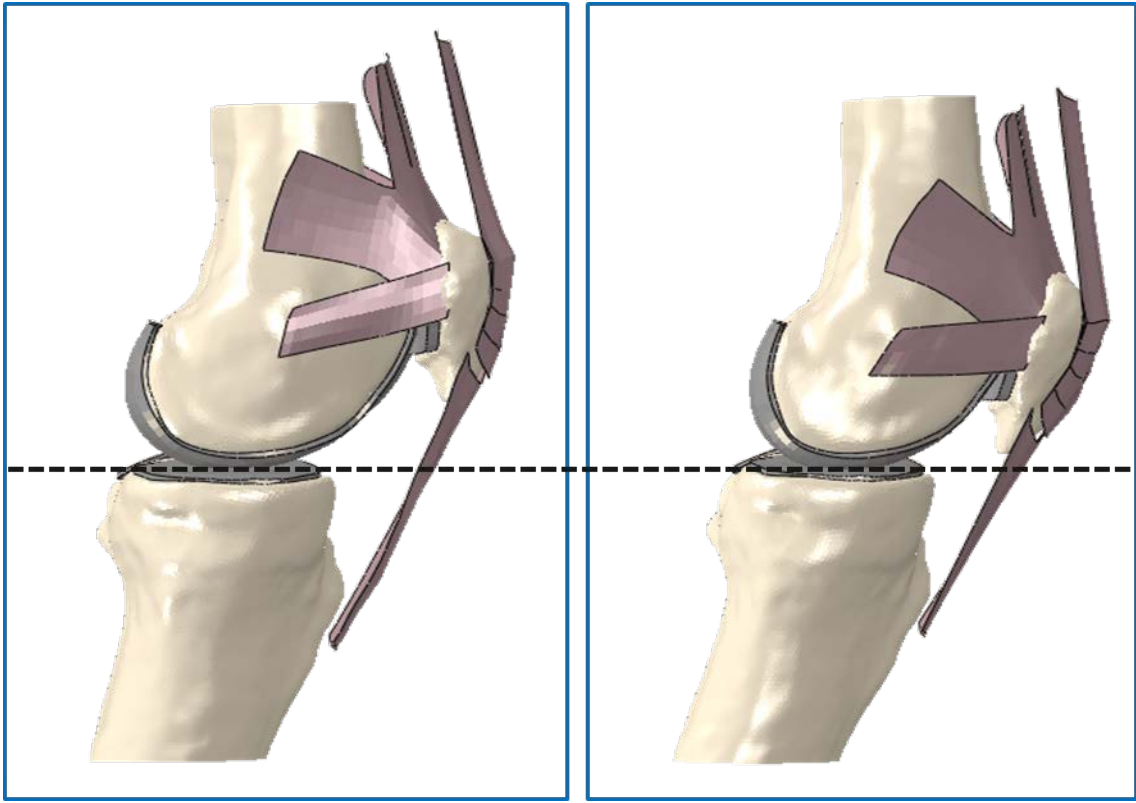


Figure 15 Pathological (left) and healthy (right) patella tendon

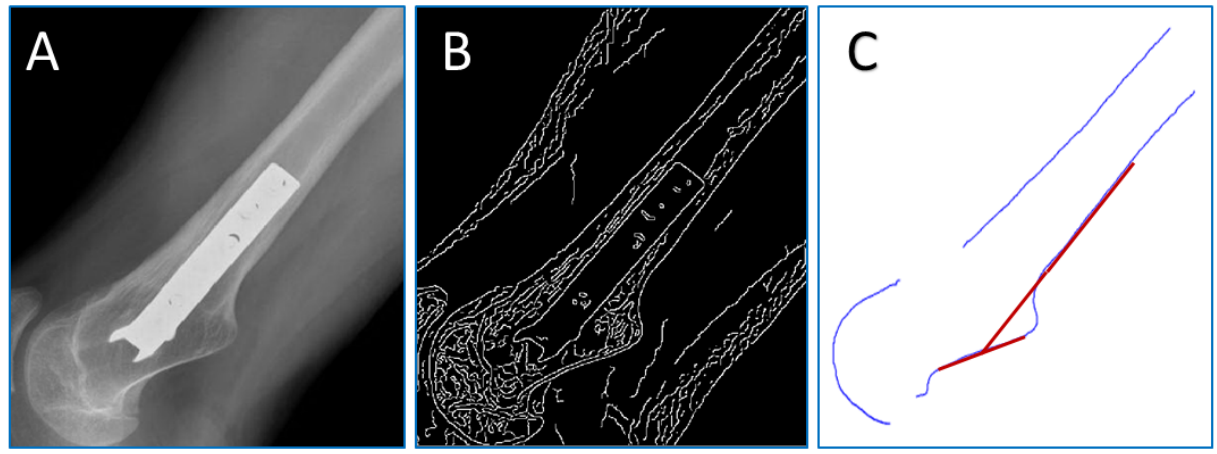


Figure 16 Radiograph after DFEO (A), edge detection (B), and lines used for baseline DFEO angle (C)

4.3 Results

The proportional-integral feedback control system used to solve for muscle forces requires the calibration of two variables for each model. The calibrated variables are the

weights assigned to proportional and integral components of the difference equations used to calculate the muscle forces. The control system is relatively simple, calculating quadriceps forces when the achieved flexion is greater than the target and hamstring forces when it's lower and otherwise enforcing a minimal muscle force for quadriceps and hamstrings (Figure 17). The calculated quadriceps and hamstring forces were divided among the corresponding muscles in the finite element model. The muscle forces act on the tibia and drive tibiofemoral flexion-extension. Unlike true muscle activation the simple control system creates highly fluctuating muscle forces where the quadriceps and hamstrings effectively take turns being active instead of finding a balance. This fluctuation in muscle forces in turn leads to oscillating kinematics. Properly calibrating the control parameters can reduce the kinematic oscillation. The root means square error between the target and achieved kinematics were calculated for each model and only those with a value of 1.5° or less were include in this study (Figure 18). For these patients, the PI controlled muscle forces were compared to the muscle forces calculated by inverse dynamics and static optimization for the models in Chapter 3 (Figure 19).

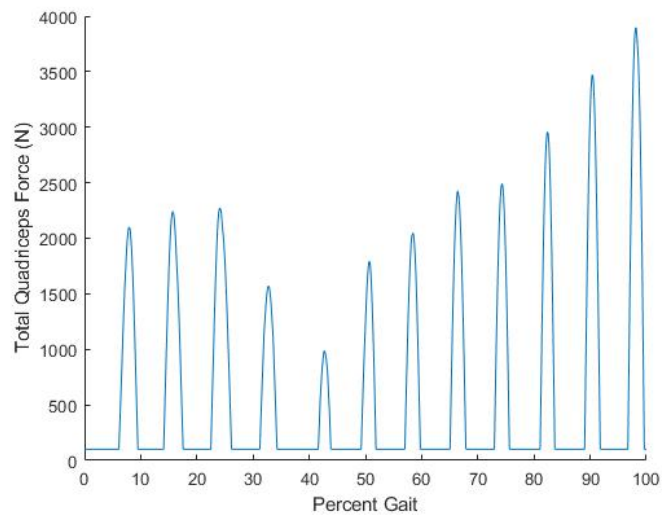


Figure 17 Total quadriceps force calculated by the proportional integral control system for a single model

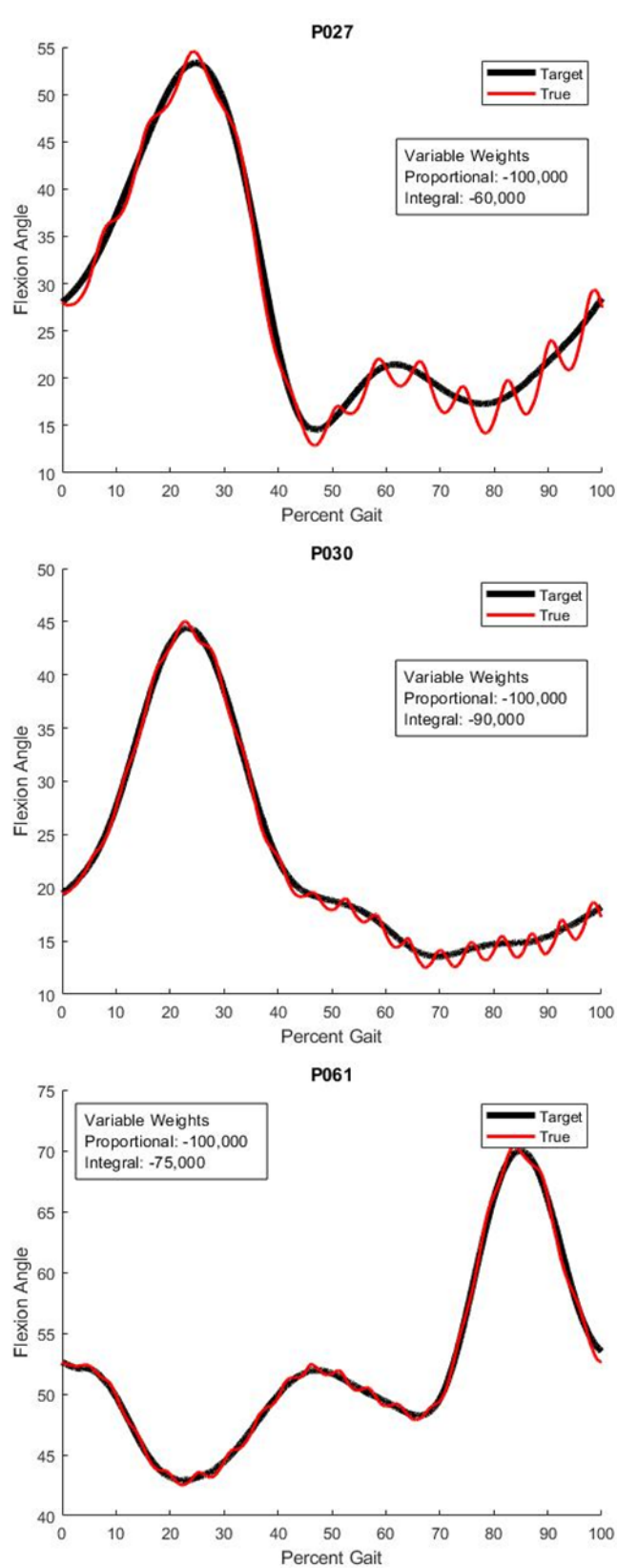


Figure 18 Target and actual tibiofemoral flexion kinematics

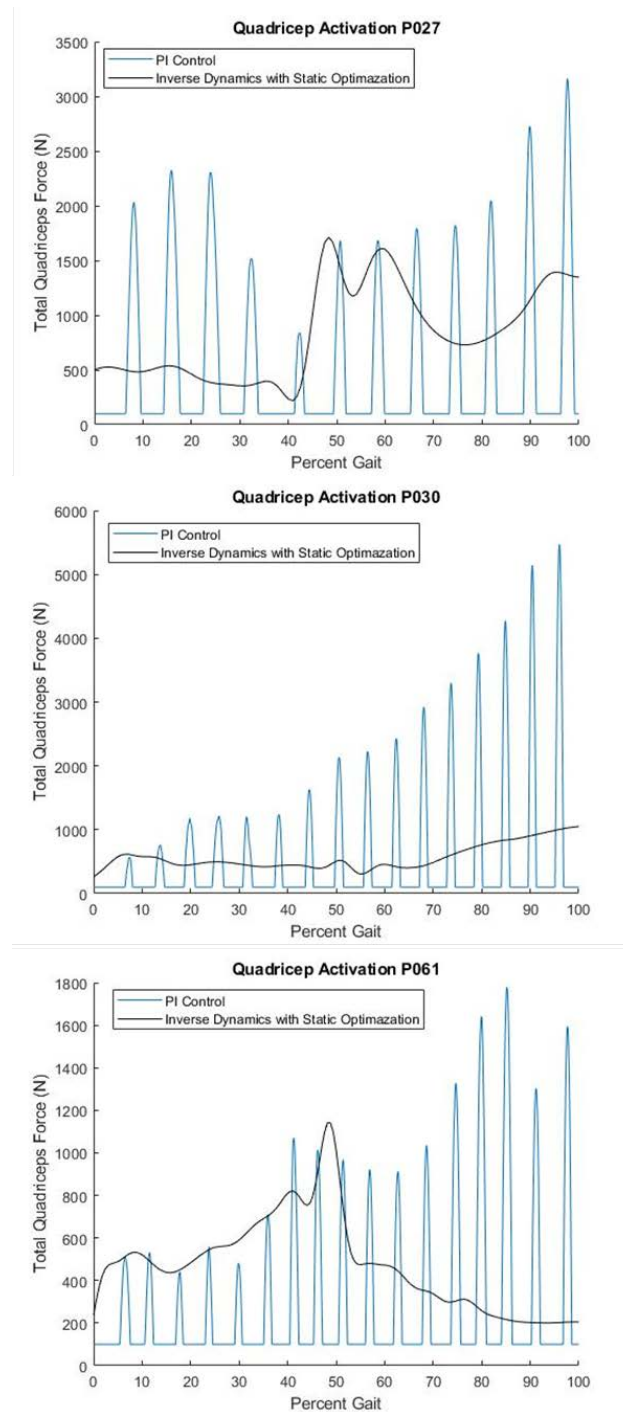


Figure 19 Total quadriceps force from PI muscle control and inverse dynamics with static optimization

The PI muscle control was successfully run for three patients each with five models with varying surgical parameters. The total quadriceps forces required for each model were compared based on surgical parameters (Figure 20). The PI muscle control

was most effective during the swing phase of gait, during stance phase the calculated muscle forces show more fluctuation due to calculation overcorrection (Figure 18). To minimize the impact of these overcorrections only muscle forces from swing phase were used for comparisons. The maximum quadriceps force from swing phase was calculated for each model. The results were compared to determine the impact of the DFEO and PTA surgeries and their associated surgical decision; angle of rotation and tendon shortening respectively.

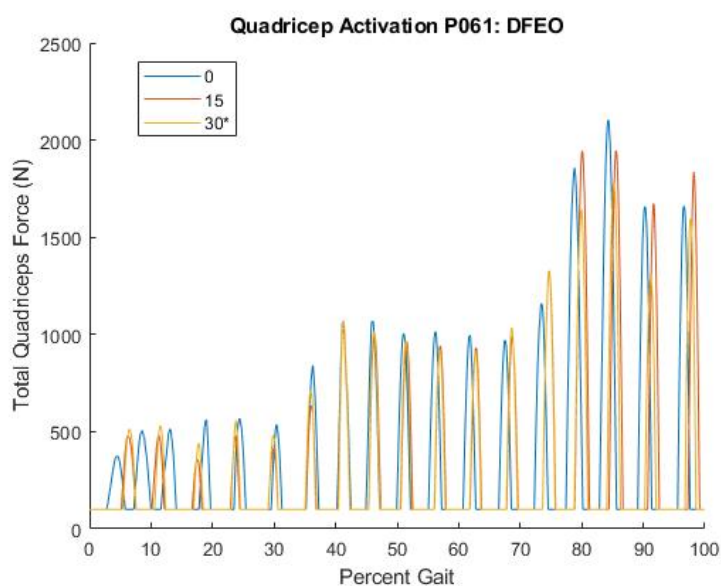


Figure 20 Total quadriceps forces for models with varying baseline DFEO angle

For the patient whose SEMLS did not include a DFEO it appears that there is a significant difference in the maximum quadriceps force of the model with 0° rotation and the models with 15° and 30° rotation. For the patient whose SEMLS surgery included a DFEO with a 15° rotation there was a significant difference in the maximum quadriceps force between the model with 30° of rotation and the models with 0° and 15° rotation. The patient whose SEMLS included a DFEO with an unknown degree of rotation showed significant difference in maximum quadriceps force between all models (Figure 21). The

initial position of each model's baseline simulation showcases the three angles of DFEO used for each model (Figure 22).

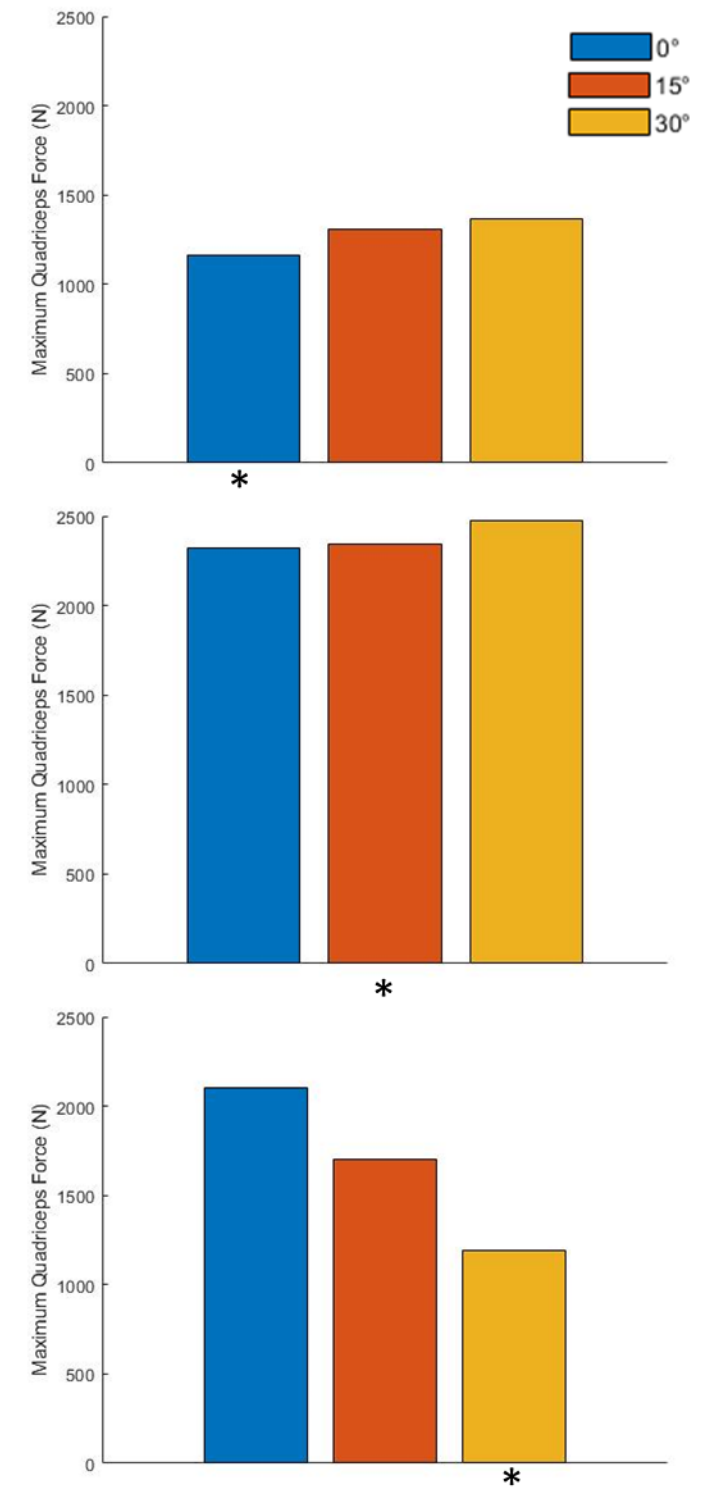


Figure 21 Maximum quadriceps force from swing phase for models with differencing DFEO angles (* indicates patient's actual surgery)

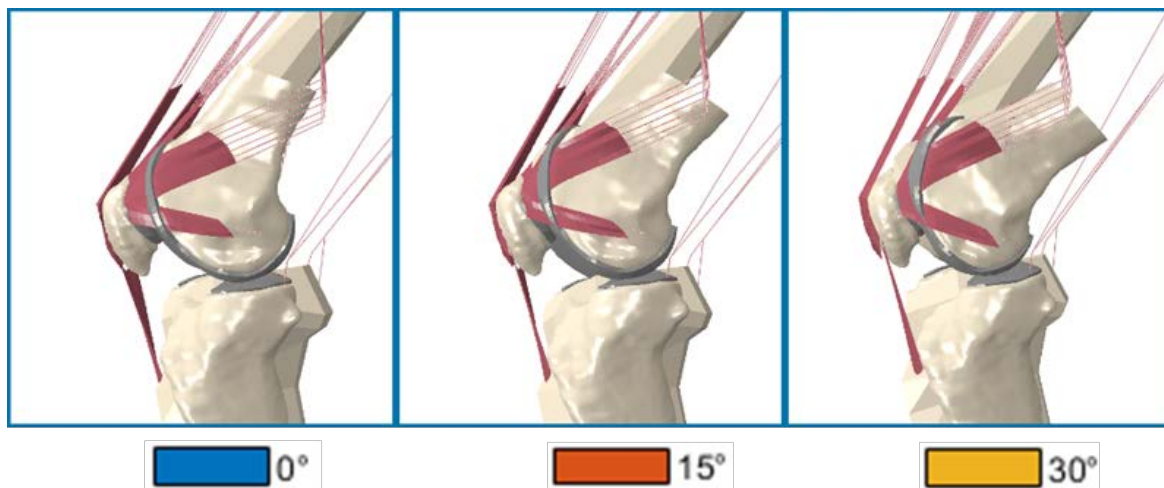


Figure 22 Initial position of knee joint for DFEO models with baseline angles; 0° (left), 15° (middle), and 30° (right)

The graphs of maximum quadriceps force were made for each model with varying patella tendon shortening (Figure 23). The initial position of the model for each variation of shortening were the same for each model, with baseline being considered the maximum shortening of 2cm (Figure 24).

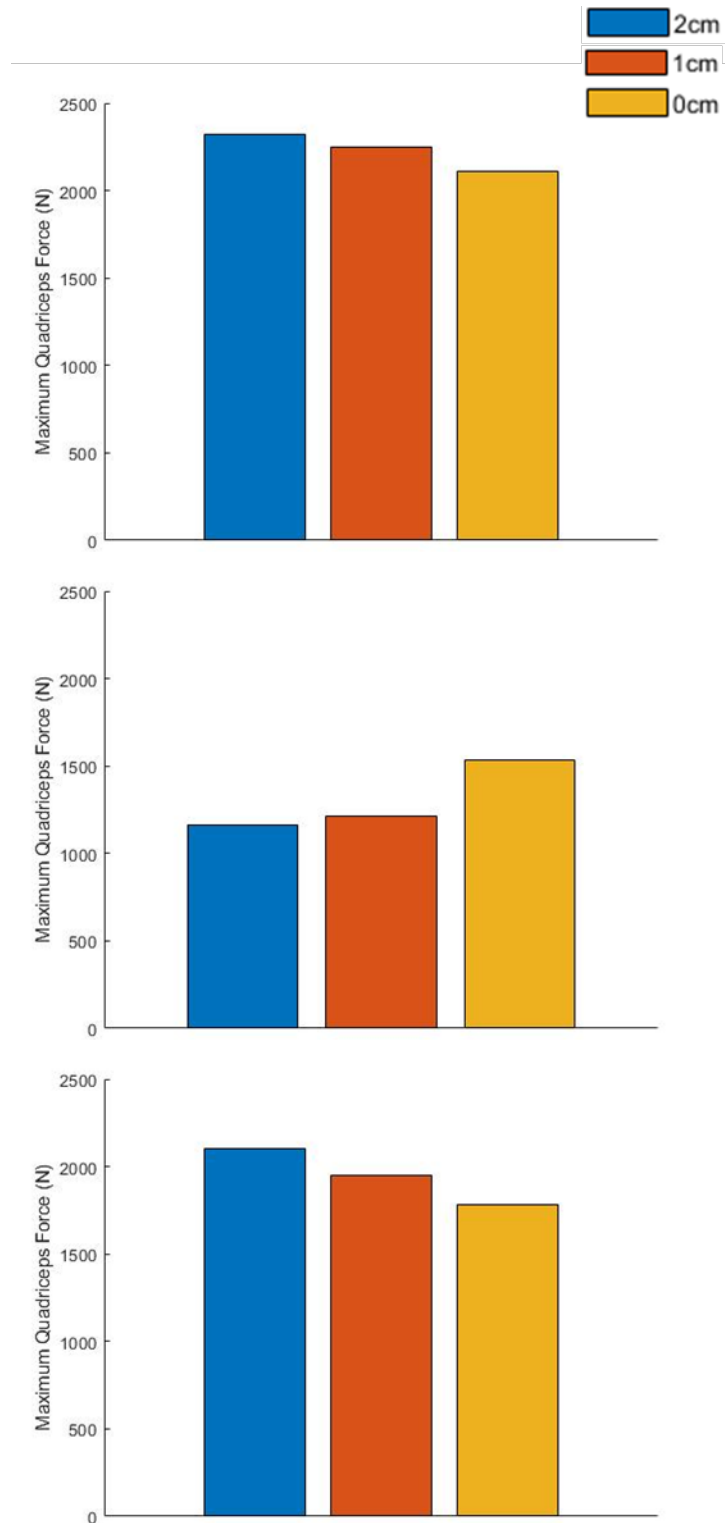


Figure 23 Maximum quadriceps force from swing phase for PTA models. Patient surgery; proximal tendon resection (top), distal tendon resection (middle), and imbrication (bottom)

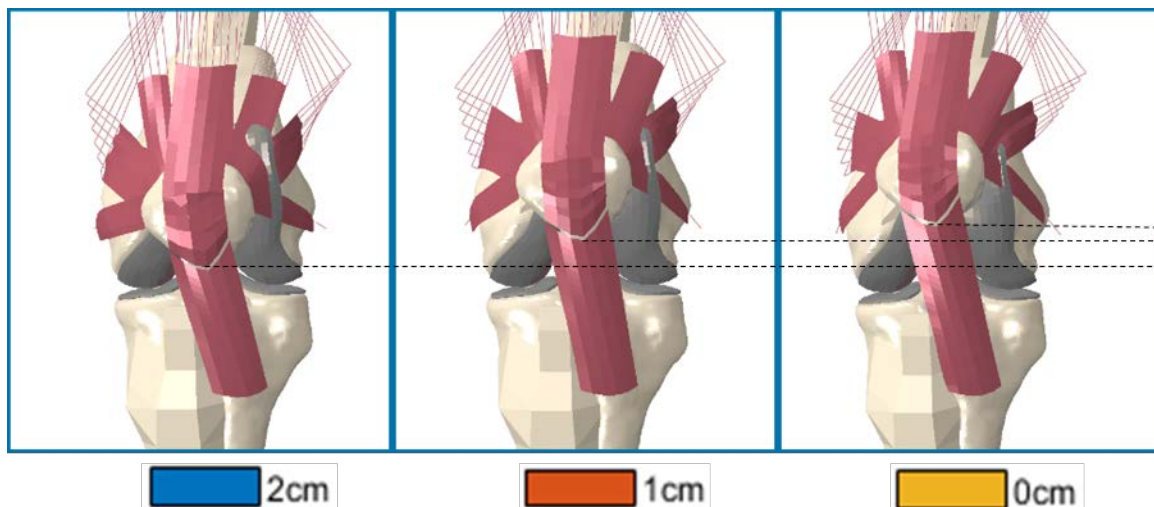


Figure 24 Initial position of knee joint for PTA models with varying lengths of Tendon Shortening; 2cm shortening (left), 1cm shortening (middle), and no shortening (right)

4.4 Discussion

The ability for the proportional-integral control system to match the target kinematics was dependent on the target profile. The control system was less capable of matching a constant target profile. When the target kinematic profile was rapidly changing, knee flexion and extension in swing phase, the achieved kinematic profile exhibited less oscillation (Figure 18). In contrast the higher levels of achieved kinematics oscillation seen in stance phase leads to greater fluctuations in muscle forces as the model struggles to maintain a relatively fixed degree of flexion (Figure 17). The current system is best suited to calculating muscle forces during the swing phase of gait when maximum flexion is achieved. The PI control system showed limited agreement with the muscle forces calculated in the earlier study using inverse dynamics and static (Figure 19).

The lower maximum quadriceps forces in the 0° model for the patient who did not have a DFEO and the higher maximum quadriceps force in the 30° model for the patient with a 15° DFEO indicate that including an unnecessary or excessive DFEO in a patient's

SEMLS will increase the difficulty of achieving natural gait kinematics. For the patient who had a DFEO with unknown rotation, the dramatic reduction in maximum quadriceps force in the model with a 15° rotation and the further reduction in the model with a 30° rotation indicate that a correctly implemented DFEO can lower the difficulty of achieving natural gait kinematics.

No clear trend emerges from the quadriceps forces of the PTA models. Further work with additional models or increasing the complexity of the muscle components used in the model may reveal a trend. Likely, the impact of PTA on quadriceps force requires is linking to subject-specific factors (limb alignment, patellar alta-baja position, muscle passive (elastic) force) that have not been accounted for in this work. However, the model development described in this analysis presents a computational testbed that may be used for further analysis and investigation.

The developed model, like all computational models, has some limitations. The proportional-integral control system used to calculate muscle forces was highly simplified. No limitations were placed on the rate of change of muscle forces creating wildly fluctuating muscle force profiles. The passive/elastic component of muscles normally present in tendons and connective tissue is unaccounted for. The model itself does not include all of the soft tissue of the knee joint that might impact tibiofemoral contact mechanics, most notable is the absence of the cruciate ligaments.

CHAPTER FIVE: CONCLUSIONS

5.1 Summary

Present literature lacks a consensus on which surgical procedures should be used to treat the underlying causes of crouch gait and there isn't a sufficient method to study the possible long-term effects of different procedures. The research aims of this thesis work were to develop a model capable of calculating both joint contact mechanics and kinematic based muscle forces and evaluate the efficacy of two surgical procedures and the impact of variations in the surgical parameters.

In the course of this research a pipeline has been developed capable of creating a lower torso finite element model with joint contact mechanics at the patellofemoral and tibiofemoral joints, tibiofemoral flexion-extension calculated by proportional-integral controlled muscles, and six degrees of freedom at eight joints (left and right hip, tibiofemoral, patellofemoral, and ankle) based on motion capture and ground reaction force data. Additionally, a system was developed to use edge detection in order to calculate patient specific surgical values, the angle of a patient's DFEO can be determined from a post-operative radiograph.

The developed model was used in a preliminary investigation into two surgical procedures but it can be refined for a more detailed study or easily adapted for additional research projects. The developed model was innovative in its combination of full lower limb musculoskeletal model and a finite element model of the knee joint with deformable cartilage. The final model had eight joints each with a full six degrees of freedom and

enough soft tissue at the knee to allow the patellofemoral joints to be entirely unconstrained. Included in this was the need to modify the accepted method for calculating kinematics to account for the incidental ML translation that results from AP rotation in a model where axes have to be physically connected to be used. The model was also able to be modified so that the flexion and extension of the tibiofemoral joint could be purely muscle-controlled using a PI control system.

5.2 Limitations

As with any computational analysis, this work involves a number of simplifications, assumptions and limitations. The accuracy of the kinematic profiles used to control the motion of the finite element model, both directly and as the target for the proportional-integral controller, was dependent on the experimental data collection and its translation first into OpenSim then Abaqus. The kinematic profiles were based on marker data but marker placement will always have variation, particularly markers placed on soft tissue like the thigh. The geometries used in each model are all scaled versions of non-pathogenic geometries, meaning that any patient specific or crouch gait pathology-specific changes to bone shape or muscle attachment location were unaccounted for. The ratio of individual muscle activation between the total force generated by the quadriceps or hamstrings is also generic, neither patient specific nor pathogenic.

Material properties also present a limitation. All soft tissue properties were ultimately based off on healthy non-pathological tissue. The patellar tendon of a subject with crouch in particular may have different properties than that of a non-pathological subject due to overstretching but no studies were found on the subject. Additionally the articular cartilage was modeled as linear elastic. Cartilage is a highly complex biphasic

material with a solid matrix phase and an interstitial fluid phase as well as varying fibril alignments based on depth. Modeling a material with that degree of complexity would be extremely computationally expensive and was ultimately beyond the scope of this study. If the cartilage was modeled more accurately I expect that stress experienced by the cartilage would be more dispersed as a result of the flow of fluid within the cartilage. It is also possible that the higher stresses of crouch gait would exasperate the biphasic creep and stress relaxation over time. The fluid phase of cartilage facilitates the low friction environment, but constant high stress can cause the fluid to leave the area of contact, increasing the stress and wear on the cartilage.

The proportional integral control system used in this study is simplistic and created muscle activation profiles that cycled between active quadriceps and active hamstrings unlike the smooth activation profile measured by electromyography (Ivaneko, Poppele, & Lacquaniti, 2004). The control system is based on the difference between the target and achieved flexion profile, with quadriceps activated when the actual angle is too flexed, and the hamstrings activated when the actual angle is too extended. This simple system creates oscillating muscle forces and kinematics and requires individual calibration for each kinematic profile. However, these models provide a framework that can be used for further investigation into surgical decision-making and patient-specific constraints.

5.3 Future Work

The model developed in the course of this research can be used in future studies and has several areas that would benefit from future improvements. The proportional integral control system used here is rudimentary and could be updated to prevent the

fluctuating muscle values currently produced. Developing a system to determine the variable weights used by the control would significantly reduce the time it takes to develop a final model for a new patient.

Updating the generic geometries used in the model would allow for research studying the effects of variable physiology. A first step might be to develop a library of geometries based on age, gender, and a variety of pathologies. This would allow for more tailored models and comparisons across certain demographics. Creating patient specific geometries would increase model accuracy but is labor intensive. Research into developing an automated system capable of segmenting articular cartilage from magnetic resonance images is currently underway (Dodin, Pelletier, Martel-Pelletier, & Abram, 2010). This type of refined computational model can be used to determine trends that simplify making surgical decisions for a wide range of pathologies. The ultimate goal would be to create a modeling system capable of providing analytical insight specific to an individual patient's situation.

REFERENCES

- Anderson, F. C., & Pandy, M. G. (2001). Static and dynamic optimization solutions for gait are practically equivalent. *Journal of Biomechanics*, *34*(2), 153-161. [https://doi.org/10.1016/s0021-9290\(00\)00155-x](https://doi.org/10.1016/s0021-9290(00)00155-x).
- Arnold, A.S., Liu, M.Q., Schwartz, M.H., Öunpuu, S., & Delp, S.L. (2006). The role of estimating muscle-tendon lengths and velocities of the hamstrings in the evaluation and treatment of crouch gait. *Gait & Posture*, *23*, 273–281. <https://doi.org/10.1016/j.gaitpost.2005.03.003>.
- Beals, R.K. (2007). Treatment of knee contracture in cerebral palsy by hamstring lengthening, posterior capsulotomy, and quadriceps mechanism shortening. *Developmental Medicine & Child Neurology*, *43*, 802–805. <https://doi.org/10.1111/j.1469-8749.2001.tb00166.x>.
- Boyer, E.R., Stout, J.L., Laine, J.C., Gutknecht, S.M., Araujo do Oliveira, L.H., Munger, M.E., Schwartz, M.H., & Novacheck, T.F. (2018). Long-Term Outcomes of Distal Femoral Extension Osteotomy and Patellar Tendon Advancement in Individuals with Cerebral Palsy. *Journal of Bone and Joint Surgery*, *100*, 31-41. <https://doi.org/10.2106/JBJS.17.00480>.
- Chang, F. M., Seidl, A. J., Muthusamy, K., Meininger, A. K., & Carollo, J. J. (2006). Effectiveness of instrumented gait analysis in children with cerebral palsy-comparison of outcomes. *Journal of Pediatric Orthopaedics*, *26*(5), 612-616. <https://doi.org/10.1097/01.bpo.0000229970.55694.5c>.
- Damiano, D.L., Laws, E., Carmines, D.V., & Abel, M.F. (2006). Relationship of spasticity to knee angular velocity and motion during gait in cerebral palsy. *Gait & Posture*, *23*, 1-8. <https://doi.org/10.1016/j.gaitpost.2004.10.007>.

- Davis III, R. B., Ounpuu, S., Tyburski, D., & Gage, J. R. (1991). A gait analysis data collection and reduction technique. *Human Movement Science, 10*(5), 575-587. [https://doi.org/10.1016/0167-9457\(91\)90046-Z](https://doi.org/10.1016/0167-9457(91)90046-Z).
- Delp, S.L., Anderson, F.C., Arnold, A.S., Loan, P., Habib, A., John, C.T., Guendelman, E., & Thelen, D.G. (2007). OpenSim: Open-Source Software to Create and Analyze Dynamic Simulations of Movement. *IEEE Transactions on Biomedical Engineering, 54*, 1940–1950. <https://doi.org/10.1109/tbme.2007.901024>.
- Dodin, P., Pelletier, J. P., Martel-Pelletier, J., & Abram, F. (2010). Automatic human knee cartilage segmentation from 3-D magnetic resonance images. *IEEE Transactions on Biomedical Engineering, 57*(11), 2699-2711. <https://doi.org/10.1002/jor.21211>.
- Fitzpatrick, C. K., Baldwin, M. A., Ali, A. A., Laz, P. J., & Rullkoetter, P. J. (2011). Comparison of patellar bone strain in the natural and implanted knee during simulated deep flexion. *Journal of Orthopaedic Research, 29*(2), 232-239. <https://doi.org/>
- Grood, E. S. & Suntay, W. J. (1983). A joint coordinate system for the clinical description of three-dimensional motions: application to the knee. *Journal of Biomechanical Engineering, 105*(2), 136-144. <https://doi.org/10.1115/1.3138397>.
- Hammer, S. R., Seth, A., Steele, K. M., & Delp, S. L. (2013). A rolling constraint reproduces ground reaction forces and moments in dynamic simulations of walking, running, and crouch gait. *Journal of Biomechanics, 46*(10), 1772-1776. <https://doi.org/10.1016/j.jbiomech.2013.03.030>.
- Harris, M. D., Cyr, A. J., Ali, A. A., Fitzpatrick, C. K., Rullkoetter, P. J., Maletsky, L. P., & Shelburne, K. B. (2016). A Combined Experimental and Computational Approach to Subject-Specific Analysis of Knee Joint Laxity. *Journal of Biomechanical Engineering, 138*(8), 081004. <https://doi.org/10.1115/1.4033882>.
- Healy, M., Schwartz, M., Stout, J., Gage, J., & Novacheck, T. (2009). Is simultaneous hamstring lengthening necessary when performing distal femoral extension

- osteotomy and patella tendon advancement? *Gait & Posture*, 30.
<https://doi.org/10.1016/j.gaitpost.2009.08.016>.
- Hicks, J.L., Schwartz, M.H., Arnold, A.S., & Delp, S.L. (2008). Crouched postures reduce the capacity of muscles to extend the hip and knee during the single-limb stance phase of gait. *Journal of Biomechanics*, 41, 960–967.
<https://doi.org/10.1016/j.jbiomech.2008.01.002>.
- Hoang, H. X. & Reinbolt, J. A. (2012). Crouched posture maximizes ground reaction forces generated by muscles. *Gait Posture*, 36(3), 405-408.
<https://doi.org/10.1016/j.gaitpost.2012.03.020>.
- Hume, D.R., Navacchia, A., Rullkoetter, P.J., & Shelburne, K.B. (2019). A lower extremity model for muscle-driven simulation of activity using explicit finite element modeling. *Journal of Biomechanics*, 84, 153-160.
<https://doi.org/10.1016/j.jbiomech.2018.12.040>.
- Ivaneko, Y.P., Poppele, R.E., & Lacquaniti, F. (2004). Five basic muscle activation patterns account for muscle activity during human locomotion. *The Journal of Physiology*, 556, 267-282. <https://doi.org/10.1113/jphysiol.2003.057174>
- Lamberts, R.P., Burger, M., Toit, J.D., & Langerak, N.G. (2016). A Systematic Review of the Effects of Single-Event Multilevel Surgery on Gait Parameters in Children with Spastic Cerebral Palsy. *Plos One*, 11.
<https://doi.org/10.1371/journal.pone.0164686>.
- Lenhart, R.L., Brandon, S.C., Smith, C.R., Novacheck, T.F., Schwartz, M.H., & Thelen, D.G. (2017). Influence of patellar position on the knee extensor mechanism in normal and crouched walking. *Journal of Biomechanics*, 51, 1–7.
<https://doi.org/10.1016/j.jbiomech.2016.11.052>.
- Lenhart, R.L., Smith, C.R., Schwartz, M.H., Novacheck, T.F., & Thelen, D.G. (2017). The effect of distal femoral extension osteotomy on muscle lengths after surgery. *Journal of Children's Orthopaedics*, 11(6), 472-478.
<https://doi.org/10.1302/1863-2548.11.170087>.

- Mo, F., Li, J., Dan, M., Liu, T., & Behr, M. (2019). Implementation of controlling strategy in a biomechanical lower limb model with active muscles for coupling multibody dynamics and finite element analysis. *Journal of Biomechanical Engineering*, *91*, 51-60. <https://doi.org/10.1016/j.jbiomech.2019.05.001>.
- Navacchia, A., Myers, C. A., Rullkoetter, P. J., & Shelburne, K. B. (2016). Prediction of in vivo knee joint loads using a global probabilistic analysis. *Journal of Biomechanical Engineering*, *138*(3), 031002. <https://doi.org/10.1115/1.4032379>.
- Naendrup, J. H., Zlotnicki, J. P., Murphy, C. I., Patel, N. K., Debski, R. E., & Musahl, V. (2019). Influence of knee position and examiner-induced motion on the kinematics of the pivot shift. *Journal of Experimental Orthopaedics*, *6*(11). <https://doi.org/10.1186/s40634-019-0183-7>.
- Novacheck, T. F., Stout, J. L., Gage, J. R., & Schwartz, M. H. (2009). Distal femoral extension osteotomy and patellar tendon advancement to treat persistent crouch gait in cerebral palsy: surgical technique. *The Journal of Bone & Joint Surgery*, *91-A*(Supplement_2), 271-286. <https://doi.org/10.1.1.875.3159>.
- Plexus Surgical Video Production. (2016, May 7). *Distal Femoral Extension Osteotomy Surgical Video* [Video File]. Retrieved from <https://www.youtube.com/watch?v=ox27ARfrj5c>
- Öunpuu, S., Solomito, M., Bell, K., Deluca, P., & Pierz, K. (2015). Long-term outcomes after multilevel surgery including rectus femoris, hamstring and gastrocnemius procedures in children with cerebral palsy. *Gait & Posture*, *42*, 365–372. <https://doi.org/10.1016/j.gaitpost.2015.07.003>.
- Rethlefsen, S.A., Blumstein, G., Kay, R.M., Dorey, F., & Wren, T.A.L. (2016). Prevalence of specific gait abnormalities in children with cerebral palsy revisited: influence of age, prior surgery, and Gross Motor Function Classification System level. *Developmental Medicine & Child Neurology* *59*, 79–88. <https://doi.org/10.1111/dmcn.13205>.
- Seidl, A., Baldini, T., Krughoff, K., Shapiro, J. A., Lindeque, B., Rhodes, J., & Carollo, J. (2016). Biomechanical Assessment of Patellar Advancement Procedures for

- Patella Alta. *Orthopedics*, 39(3), 492-497. <https://doi.org/10.3928/01477447-20160427-04>.
- Sossai, R., Vavken, P., Brunner, R., Camathias, C., Graham, H.K., & Rutz, E. (2015). Patellar tendon shortening for flexed knee gait in spastic diplegia. *Gait & Posture* 41, 658-665. <https://doi.org/10.1016/j.gaitpost.2015.01.018>.
- Stout, J.L., Gage, J.R., Schwartz, M.H., & Novacheck, T.F. (2008). Distal Femoral Extension Osteotomy and Patellar Tendon Advancement to Treat Persistent Crouch Gait in Cerebral Palsy. *The Journal of Bone and Joint Surgery-American Volume* 90, 2470–2484. <https://doi.org/10.2106/jbjs.g.00327>.
- Yeargin-Allsopp, M., Braun, K.V.N., Doernberg, N.S., Benedict, R.E., Kirby, R.S., & Durkin, M.S. (2008). Prevalence of Cerebral Palsy in 8-Year-Old Children in Three Areas of the United States in 2002: A Multisite Collaboration. *Pediatrics* 121, 547–554. <https://doi.org/10.1542/peds.2007-1270>.
- Yu, B., Gabriel, D., Noble, L., & An, K.N. (1999). Estimate of the optimum cutoff frequency for the Butterworth low-pass digital filter. *Journal of Applied Biomechanics*, 15(3), 318-329. <https://doi.org/10.1123/jab.15.3.318>.